Osteology and Systematics of *Parastromateus niger* (Perciformes: Carangidae), with Comments on the Carangid Dorsal Gill-Arch Skeleton

Eric J. Hilton[1], G. David Johnson[2], and William F. Smith-Vaniz[3]

The monotypic Indo-Pacific genus *Parastromateus* Bleeker, 1864 is morphologically peculiar among carangid fishes in its overall body form and has been difficult to place phylogenetically. This has been partly the result of a lack of detailed morphological data for this and other carangid fishes. Here, we describe and analyze the osteology of *Parastromateus niger* (Bloch, 1795), review its taxonomic history, and describe characters that are suggestive of its phylogenetic affinities. In addition, we made a broad survey of gill-arch skeletal characters for carangids. Previous studies have noted that a combination of features from the skeletal anatomy of *Parastromateus* firmly places it within the Carangidae (presence of a gap between the second and third anal-fin spine) and within the tribe Carangini (presence of scutes, inferior vertebral formina). Within the Carangini, however, its phylogenetic placement is less clear. In our survey of the gill arches of Carangidae, we found that only *Parastromateus* and *Hemicaranx* have an enlarged toothplate that bridges the epibranchial 4–ceratobranchial 4 joint. Additionally, these two genera have a superficially similar form of teeth on the pharyngeal toothplates (elongate and filamentous vs. conical and stout in other carangins). Although outside the scope of our study, these and other morphological aspects of *Parastromateus* need to be brought into a broad-based cladistic analysis of the Carangidae.

T HE family Carangidae (jacks, trevallies, pompanos, and their relatives) comprise about 140 species classified in 32 genera of marine percomorphs distributed worldwide in temperate and tropical oceans (Nelson, 2006). Many carangids are popular game fishes and as a group have a remarkably diverse array of adult body forms, ranging from slender, streamlined (*Decapterus*, *Megalaspis*, and *Elagatis*) to deep-bodied (*Alectis* and *Selene*), to large and blunt-headed (some species of *Caranx*). Detailed osteologies are available for some carangid species (Suda, 1996) as are useful comparative anatomical studies (Starks, 1911; Suzuki, 1962), but detailed morphological (including osteological) data are lacking for most taxa within the family. Here we attempt to remedy this lack of osteological data for the taxonomically problematic monospecific genus, *Parastromateus* Bleeker, 1864.

Parastromateus niger (Bloch, 1786), the Black Pomfret, is distributed along the continental shelf throughout the Indian and western Pacific Oceans, ranging from the coast of South Africa east through Indonesia to Queensland, Australia and the southern coast of Japan and China (de Beaufort and Chapman, 1951; Witzell, 1978; Pati, 1983; Smith-Vaniz, 1999). Large schools of *P. niger* have been observed with individuals swimming on their sides (Smith-Vaniz, 1999). *Parastromateus* also makes a daily vertical migration from muddy bottoms (15–40 m in depth), where it spends its days, to the surface at night, presumably to feed on zooplankton (Smith-Vaniz, 1999). Planktonic crustaceans, primarily copepods and brachyuran zoeae, were the most common food items of *Parastromateus* in Kuwaiti waters (Dadzie, 2007), but fish eggs, scales, and phytoplankton were also major components in the diet. Dadzie et al. (2000) and Pati (1980) established that *Pampus argenteus*, a superficially similar stromateid, exploits nearly identical food resources.

Parastromateus is a deep-bodied fish that attains at least 55 cm fork length (Fig. 1; Smith-Vaniz, 1986). The dorsal and anal fins are nearly mirror images of one another, and the pelvic fins, which are well developed in juveniles, disappear externally by about 90 mm standard length (Witzell, 1978). Its overall gestalt is reminiscent of stromateoids (Doiuchi et al., 2004), leading to both its common and generic names, and to some extent, the confusing history of its taxonomic placement. Haedrich (1967:51) considered the possibility that the genus is somehow related to the stromateoids, but concluded, "Even if *Parastromateus* is related to the stromateids, the relationship is at most a very distant one." Smith-Vaniz (1984) demonstrated that *Parastromateus* belongs within the Carangidae because of the separation of the second and third anal-fin spines, which he hypothesized as a synapomorphy of the family (also Gushiken, 1988, although this character may be more complicated than presented in the literature and include other aspects of the form of the spines, such as their relative length, as this gap is seen in a number of other perciforms, such as *Pomatomus* and priacanthids; V. G. Springer, pers. comm., 2008). In previous studies of *Parastromateus*, Apsangikar (1953), Witzell (1978), and others have emphasized its external anatomy. Le Danois (1963) provided a description of some aspects of its osteology and myology. Deng and Zhan (1986) and Deng et al. (1985) described and illustrated the lateral line system of *Parastromateus*. Yamada and Nakabo (1986) provided the most comprehensive review of the anatomy of this genus to date. Smale et al. (1995) gave detailed descriptions and illustrations of the otoliths of *Parastromateus* and other carangids. Springer and Smith-Vaniz (2008) provided extensive data and illustrations of portions of the axial skeleton of *Parastromateus* in the context of their study of supraneural and pterygiophore insertion patterns of carangids and other acanthomorphs.

[1] Virginia Institute of Marine Science, College of William and Mary, Gloucester Point, Virginia 23062; E-mail: ehilton@vims.edu. Send reprint requests to this address.
[2] Department of Zoology, Division of Fishes, Smithsonian Institution, P.O. Box 37012, National Museum of Natural History, MRC 0159, Washington, D.C. 20013-7012; E-mail: johnsond@si.edu.
[3] Florida Museum of Natural History, Dickinson Hall, Museum Road, University of Florida, Gainesville, Florida 32611-7800; E-mail: smithvaniz@gmail.com.
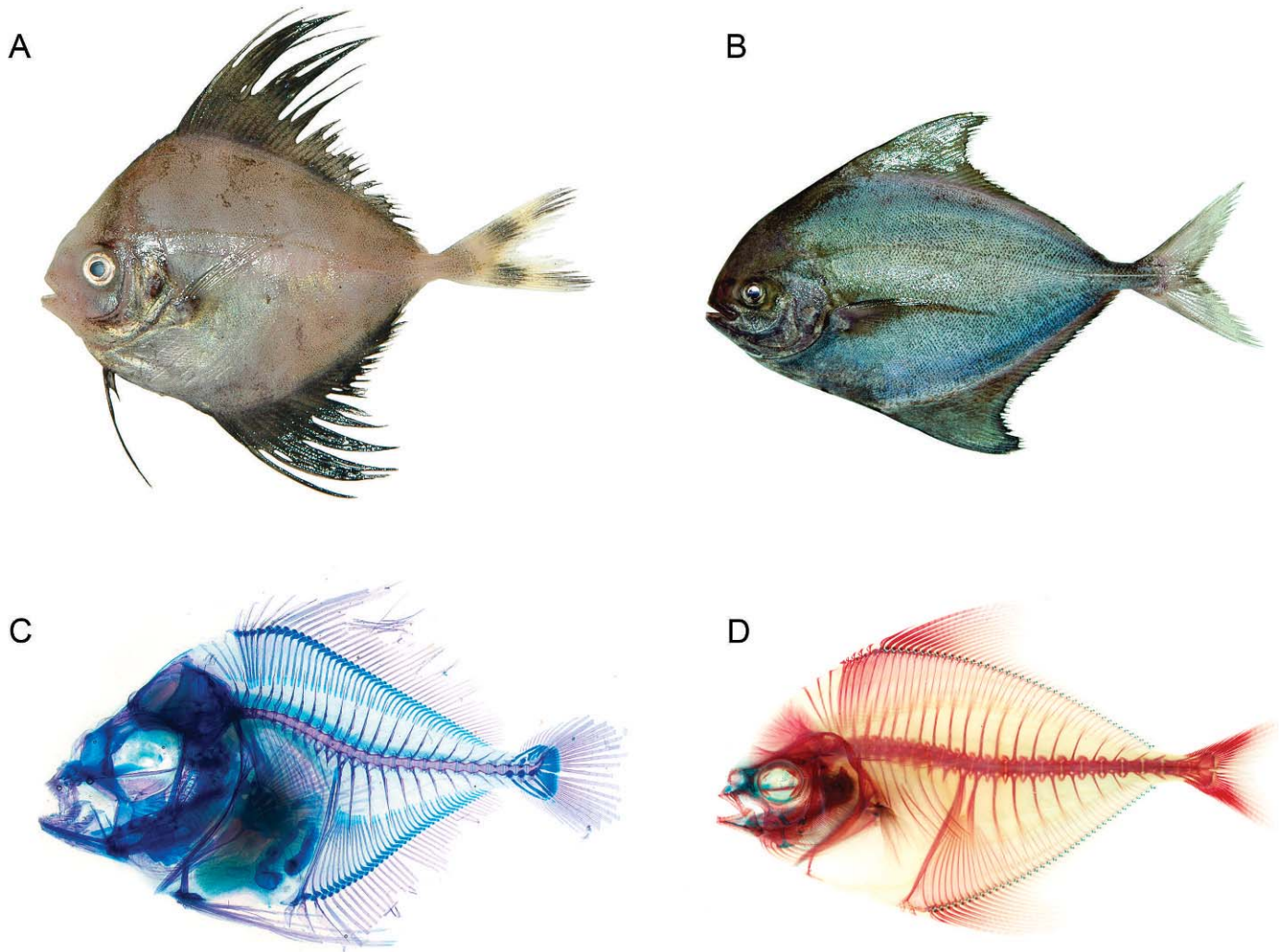
Fig. 1. *Parastromateus niger*. (A) Fresh juvenile specimen (ASIZP 66167, 88 mm SL, Taiwan). (B) Fresh adult specimen (ASIZP 65880, 261 mm SL, Taiwan). (C) Cleared-and-stained larva (USNM 388226, 11 mm SL). (D) Cleared-and-stained skeleton (ANSP 62088, 100 mm SL). Anterior facing left. (A) and (B) from K. T. Shao. The Fish Database of Taiwan. WWW Web electronic publication, version 2005/5 http://fishdb.sinica.edu.tw.

In this paper, we describe and illustrate the skeletal anatomy of *Parastromateus niger* based primarily on cleared-and-stained specimens. This study began as a survey of the gill-arch skeleton of carangid fishes to determine the level of phylogenetic variation within this family of this understudied character system. We found that the gill-arch skeleton of *Parastromateus* is peculiar among carangids. Given the paucity of osteological information for *Parastromateus* in the literature, we expanded the study to include the entire skeleton. We also describe and illustrate the comparative osteology of the dorsal gill arches of carangid fishes. We summarize the taxonomic history of *P. niger* and consider its systematic affinities within the family Carangidae, highlighting derived characters found in its gill-arch skeleton.

MATERIALS AND METHODS

Five cleared-and-stained, 19 dry skeletal, and 18 whole alcohol-preserved specimens were examined in this study. Cleared-and-stained specimens were prepared following the methods of Dingerkus and Uhler (1977). According to Pati (1983), *P. niger* matures at between 280 (male) and 300 mm SL (female). The cleared-and-stained specimen that serves as

the basis for most of our illustrations (120 mm SL) is therefore immature. However, we also studied dry skeletons of mature and nearly mature specimens (based on their size), and no significant differences in the morphology of the cleared-and-stained and dry skeleton specimens were noted. Radiographs were used to collect meristic data from several alcohol-preserved specimens. Line drawings were rendered using Adobe Illustrator software based on camera lucida sketches. Institutional abbreviations are as listed at http://www.asih.org/codons.pdf.

RESULTS

Skull roof and neurocranium.—The surface of most of the bones of the skull have a fibrous texture that obscures many of the sutures, particularly those that are deeply interdigitating. Paired parietals, pterotics, epioccipitals, and the median supraoccipital form much of the posterior portion of the skull roof; only a small portion of the intercalar is visible in dorsal view. In lateral view, the neurocranium is remarkably deep, owing to a large supraoccipital crest that reaches far anteriorly (Fig. 2). The supraoccipital crest is continuous anteriorly with a median crest formed by anterodorsal extensions of the frontals. On either side of the crest formed
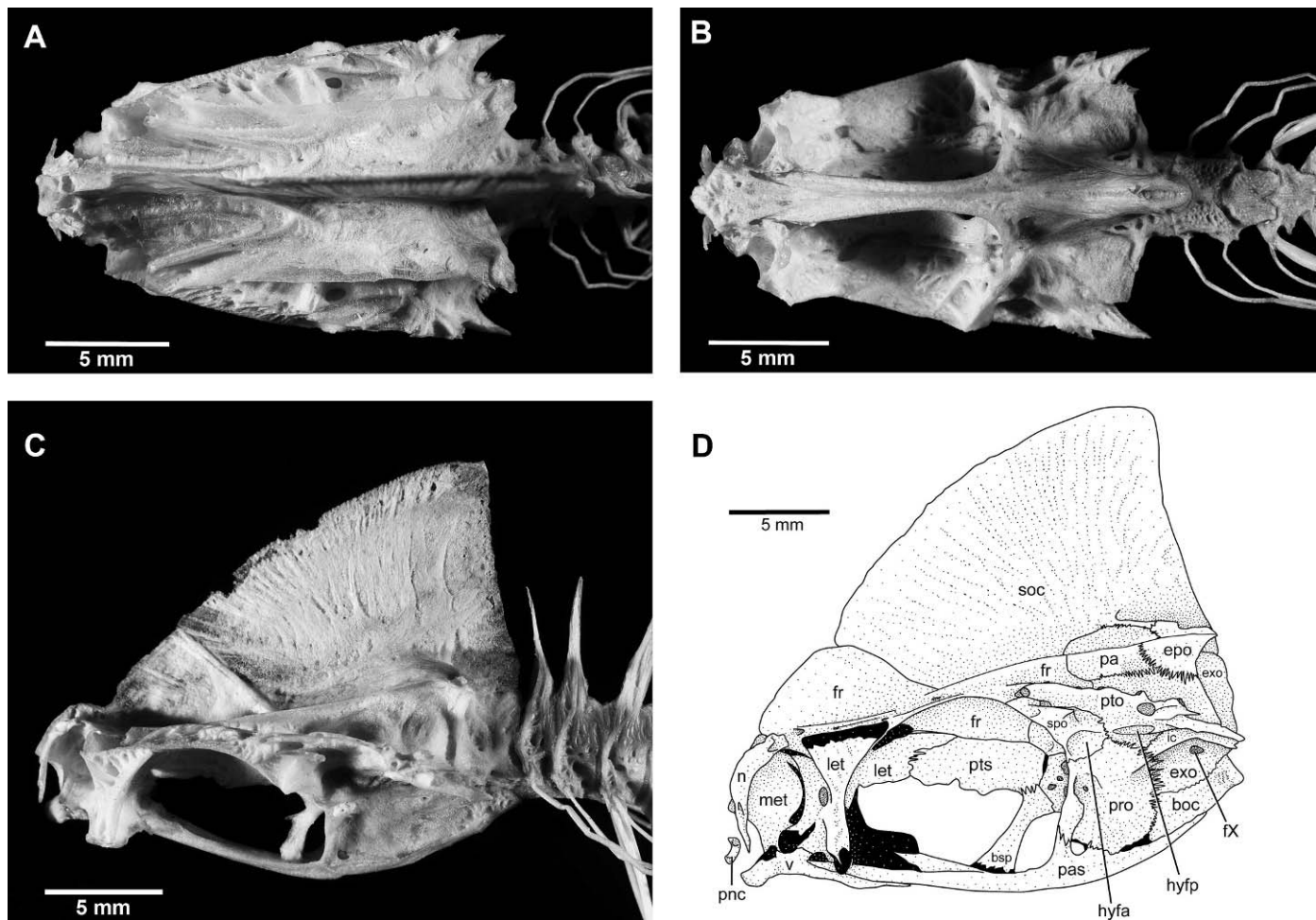
Fig. 2. Photographs of the skull roof and neurocranium of *Parastromateus niger* in (A) dorsal, (B) ventral, and (C) left lateral views (AMNH 98949, est. 185 mm SL). (D) Line drawing of skull roof and neurocranium in lateral view (ANSP 62088, 120 mm SL). Anterior facing left. Bone in stipple, cartilage in black. Abbreviations: boc, basioccipital; bsp, basisphenoid; epo, epioccipital; exo, exoccipital; fr, frontal; fX, foramen for the vagus nerve; hyfa, anterior facet for hyomandibula; hyfp, posterior facet for hyomandibula; ic, intercalar; let, lateral ethmoid; met, mesethmoid; n, nasal; pa, parietal; pnc, prenasal canal bone; pro, prootic; pto, pterotic; pts, pterosphenoid; soc, supraoccipital; spo, sphenotic; v, vomer.

by the frontals, each bone has a flattened surface that supports the supraorbital sensory canal, which bears several lateral branches contained in the frontals. The nasal bone is a simple tube that curves gently around the anterior margin of the nasal capsule. Ventral to the nasal is the small tubular prenasal canal bone (Fig. 2D), which is characteristic of Carangoidei (Freihofer, 1978; Johnson, 1984).

On either side of the supraoccipital crest are two bony ridges on the skull roof: a lateral one formed primarily by the pterotic, and a medial one formed by the frontal, parietal, and epioccipital. The lateral ridge arises in the frontal at the level of the posterior portion of the orbit and continues posteriorly along the entire lateral margin of the pterotic, rising slightly dorsally. The medial one begins further anteriorly (above the anterior portion of the orbit) and ends posteriorly, blending into the flattened region of the epioccipital that forms the articular surface for the dorsal arm of the posttemporal. These ridges demarcate a pair of deep troughs immediately on either side of the frontal and supraoccipital crests, as well as a pair of more lateral troughs along the lateral margins of the skull roof (Fig. 2).

The extrascapular (not illustrated) carries the sensory canal a short distance from the posttemporal to the pterotic and dorsally at the level of the posterior margin of the

supraoccipital crest, curving slightly posteriorly as it approaches the dorsal margin of the head. The pterotic carries the otic sensory canal along its dorsolateral margin. This canal contains several branches that exit laterally along the apex of the lateral ridge on the skull roof. Ventrally, the pterotic bears the articular surface for the posterior dorsal head of the hyomandibula. The articular surface for the anterior dorsal head of the hyomandibula is entirely within the sphenotic, which lies dorsal to the prootic and the pterosphenoid and posterior to the frontal. The paired prootic is the largest bone of the lateral wall of the neurocranium, and has a well-defined bridge of bone defining the trigeminofascialis chamber. The massive pterosphenoid contacts the posterior extension of the lateral ethmoid anteriorly, the frontal and sphenotic dorsally, and the basisphenoid and prootic posteriorly (Fig. 2D). The basisphenoid extends anteroventrally from its suture with the pterosphenoids and prootics to contact the parasphenoid (through cartilage) at the posterior extent of the median dorsal lamina of the parasphenoid (Fig. 2D). *Parastromateus* is unusual among carangids, as it is the only known taxon with a non-pattern-10 *ramus lateralis accessorius* (Friehofer, 1963) and to possess a *pons moultoni*, a bridge of bone associated with the anterior vertical canal of the

inner ear (Haedrich, 1971; see Johnson and Fritzsche, 1989 for further discussion of this character). However, because both characters are difficult to observe, these character states (both generally considered to be plesiomorphic) have not been surveyed in many carangid genera.

The paired intercalars contact the exoccipitals, prootics, and the posteroventral surfaces of the pterotics and receive the stout ventral arms of the posttemporals. Together the paired exoccipitals and the median basioccipital form a tripartite occipital condyle. The first centrum bears two posteriorly directed ventrolateral processes that articulate with the second centrum, resulting in a seemingly movable joint (Fig. 2B; fresh specimens were not available for manipulation, although other carangids, e.g., *Selene vomer*, have a similar complex articulation that allows considerable movement of the skull relative to the anteriormost vertebra).

The ethmoid cartilage supports the endochondral median ethmoid and paired lateral ethmoids, and the closely associated median dermal vomer. The lateral surfaces of the median ethmoid are concave and form the internal surfaces of the nasal capsules. The lateral ethmoids form the posterior walls of the nasal capsules. Each lateral ethmoid bears a lateral triangular wall that extends ventrally to form a rounded cartilaginous prominence. Ventrally, the lateral ethmoids broadly contact the dorsal surface of the vomer. The ventral margin of the vomer is slightly concave in lateral view. The vomer broadly contacts the ethmoid cartilage on its anterior half, and posteriorly is overlapped by the anterior end of the parasphenoid. In lateral view, the parasphenoid is slightly convex ventrally and contacts the vomer anteriorly, the basisphenoid at its midpoint, and the prootic and basioccipital posteriorly. There is a dorsal median lamina of bone on the anterior portion of the parasphenoid that becomes entirely embedded in the ethmoid cartilage anteriorly. The parasphenoid contacts the prootic: posteriorly through a cartilage-filled suture and anteriorly through a shallow ascending process that is sutured to an anterolateral arm of the prootic to form the trigeminofacialis canal. Posteriorly, the parasphenoid smoothly contacts the ventral surface of the basioccipital near the point at which Baudelot's ligament connects to the skull.

Infraorbital bones and sclerotic ring.—The infraorbital series consists of six ossifications, including five infraorbitals plus the dermosphenotic (Fig. 3). The dermosphenotic is by far the smallest of all the infraorbital bones and is little more than an ossification of the tube defining the sensory canal. Infraorbital one, in contrast, is the largest of the series and is positioned just ventral and lateral to the lateral ethmoid. Infraorbitals 2 and 3 are similar to each other in overall size, as are infraorbitals 4 and 5. The subocular shelf extends from the medial surface of the anterior portion of infraorbital 3 (''second suborbital'' of Suzuki, 1962). Gushiken (1988:character 13) found that one of the two characters that separated *Parastromateus* morphologically from all other carangins was the absence of posteriorly directed process from the subocular shelf that is found in all others. However, we found that the shelf and process is formed in *Parastromateus* as in other carangins, although there is individual variation in its shape.

The sclerotic cartilage supports two ossifications, positioned anteriorly and posteriorly in the orbit. These bones
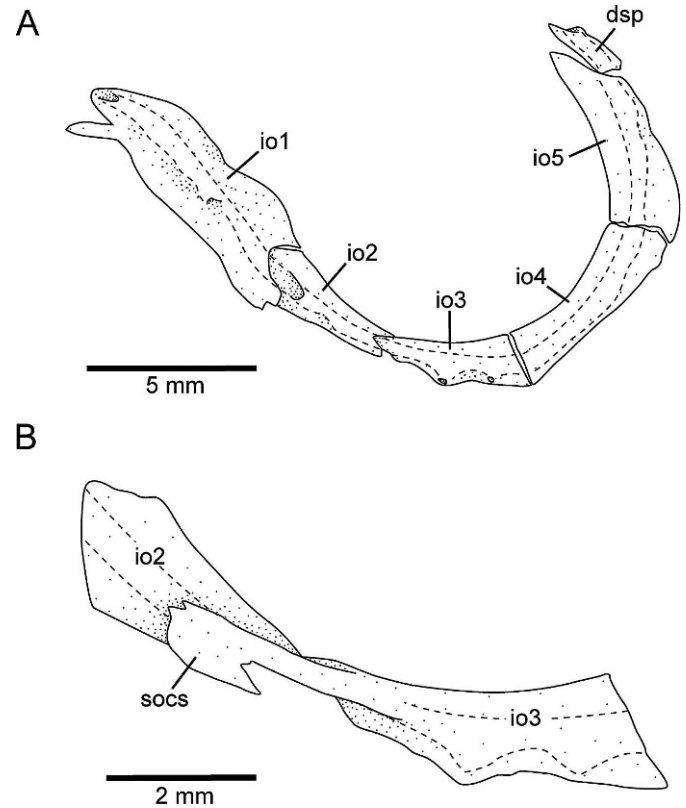

Fig. 3. Infraorbital series of *Parastromateus niger* (ANSP 62088; 120 mm SL). (A) Left infraorbital bones in lateral view. (B) Medial view of io2 and io3 showing subocular shelf. Anterior facing left (in B, image flipped). Dashed line indicates course of sensory canals. Abbreviations: dsp, dermosphenotic; io, infraorbital; socs, subocular shelf.

are relatively robust and contact each other dorsally and ventrally at the midpoint of the eye.

Opercular bones, suspensorium, and jaws.—The opercular bones are all thin (although well-ossified) dermal bones that dissipate along their free edges into the skin, so as to give a ragged appearance to their free margins (Fig. 4A, B). The opercle is roughly triangular in shape with a distinct notch in its posterodorsal margin. A similar notch is also present in many other carangids (Suzuki, 1962:figs. 18–27). The anterodorsal corner of the opercle is drawn out dorsally into a process that is positioned dorsal and lateral to the opercular facet. Medially, there is also a process on the opercle that is continuous with the opercular facet. The subopercle is roughly V-shaped, with an exaggerated posterior arm that is over half the length of the opercle. The subopercle is positioned medial to both the opercle and the broad, rectangular interopercle, which extends anteriorly from the ventral point of the opercle. Although part of the opercular series, the branchiostegals are described in the section *Ventral portion of the hyoid arch* because of their close association with that part of the visceral skeleton. The preopercle has a very narrow vertical limb that is not much broader than the width of the sensory canal it supports. The preopercular sensory canal, which bends anteriorly at an almost 90° angle, opens from the preopercle on its horizontal limb through a series of pores. Although the horizontal and vertical limbs of the preopercle are distinct, the anterior margin of the bone is smoothly arched.
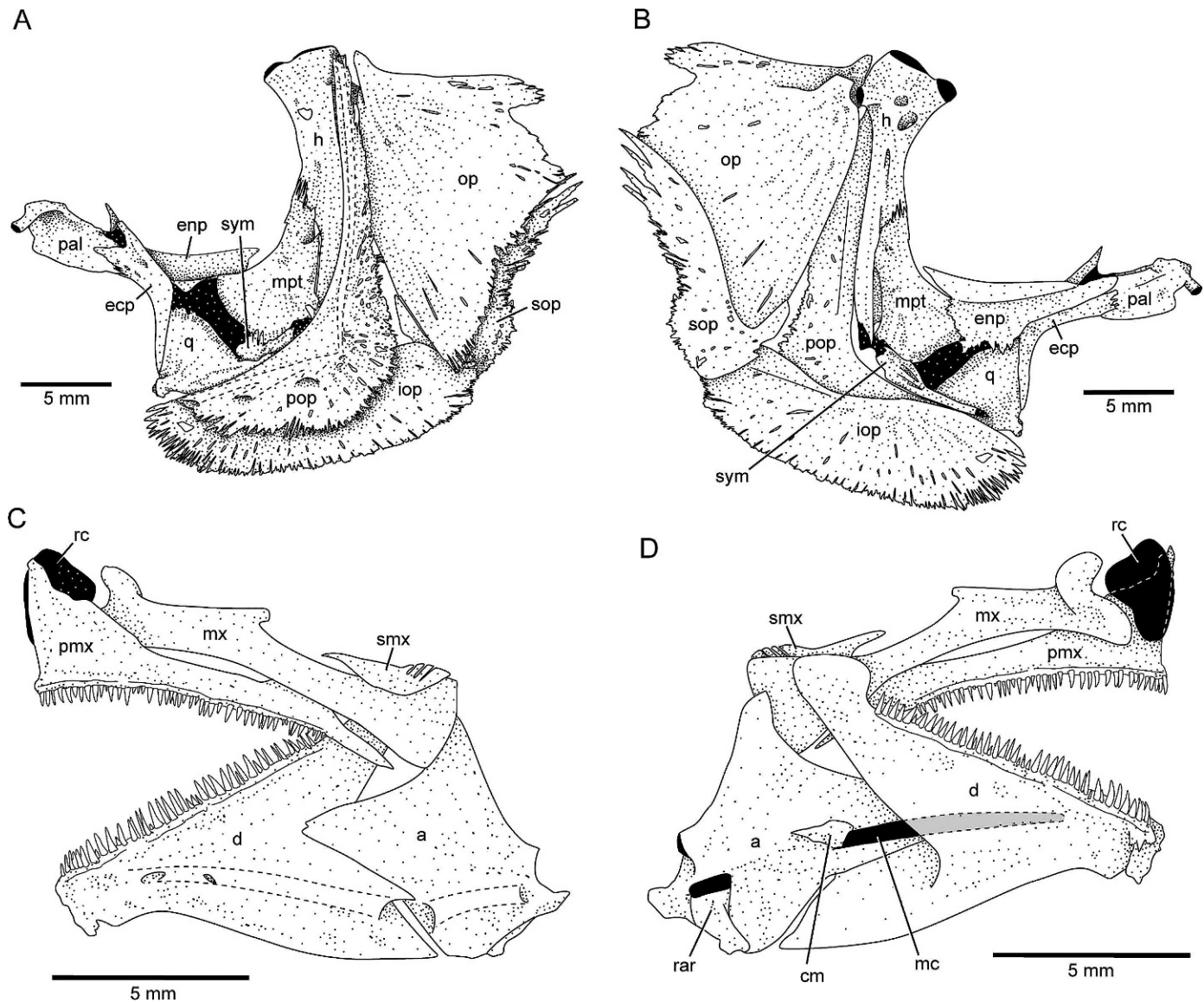
Fig. 4. Suspensorium, opercular bones, and oral jaws of *Parastromateus niger* (ANSP 62088, 120 mm SL). (A) Lateral view of suspensorium and opercular bones; anterior facing left. (B) Medial view of suspensorium and opercular bones; anterior facing right. (C) Lateral view of oral jaws; anterior facing left. (D) Medial view of oral jaws; anterior facing right. Bone in stipple, cartilage in black; dashed line indicates course of sensory canals; gray in (D) indicates portion of Meckel's cartilage inside dentary. Abbreviations: a, anguloarticular; cm, coronomeckelian; d, dentary; ecp, ectopterygoid; enp, endopterygoid; h, hyomandibula; iop, interopercle; mc, Meckel's cartilage; mpt, metapterygoid; mx, maxilla; op, opercle; pal, palatine; pmx, premaxilla; pop, preopercle; q, quadrate; rar, retroarticular; rc, rostral cartilage; smx, supramaxilla; sym, symplectic.

The hyomandibula is very slender and bears two articular surfaces for contact with the neurocranium. The opercular condyle is small and is almost completely hidden in lateral view by the opercle and preopercle. The hyomandibula contacts the metapterygoid anteroventrally at about its midlength, and ventrally it is continuous with the symplectic through the remnant of the hyosymplectic cartilage. The symplectic lies dorsal to the posteroventral process of the quadrate. The symplectic is almost completely hidden in lateral view anteriorly and is much more slender than the robust posterior portion, which overlaps the ventral margin of the metapterygoid laterally through fingers of membrane bone that grow dorsally.

The metapterygoid contacts the hyomandibula through much of its posterior margin and posterodorsally tightly sutures to the hyomandibula. Laterally, the metapterygoid bears a prominent flange-like process. The quadrate has a

triangular body and bears a prominent posteroventral process that is closely associated with the symplectic. Anteroventrally, the quadrate has a broad articular condyle for the lower jaw joint. The main portions of the ectopterygoid and the endopterygoid contact one another for most of their lengths (Fig. 4B). The endopterygoid has a dorsal shelf, which laterally follows the cartilage of the palatoquadrate, whereas medially it becomes thin and supports the orbit. The suborbital shelf of infraorbital 3 contacts the base of the endopterygoid. The ectopterygoid defines the lateral margin of the posterior portion of the anterior half of the palatopterygoid. It is distinctly bent at an angle approaching 90°. Anteriorly, both the ectopterygoid and the endopterygoid contact the posterior end of the palatine. The palatine is a complexly shaped bone, with a ventromedial flange along most of its length and a distinct anterolateral process. The cartilage-capped anterolateral

palatine process articulates with the lateral ethmoid and then curves ventrally to articulate with the dorsal surface of the maxilla.

The premaxilla has a well-developed ascending process that is tightly associated with the rostral cartilage (Fig. 4C, D). A single row of small conical teeth is present on its ventral margin for most of its length; the narrow edentulous portion of the premaxilla overlaps the lower jaw laterally. There are 42 teeth on the right premaxilla in the single specimen we counted (UF 168246). Posteriorly, the premaxilla is drawn out into a sharp point. The maxilla is broadest posteriorly. Anteriorly, the maxilla curves dorsomedially where it articulates with the premaxilla, and bears a distinct dorsal process that articulates with the posterior region of the rostral cartilage (Fig. 4C, D). At about its midlength, the maxilla bears a posteriorly directed process on its dorsal margin for attachment of the adductor mandibulae. The supramaxilla slightly overlaps the maxilla laterally and is more weakly ossified dorsally than it is ventrally, where it contacts the maxilla.

The dentary has a single row of small and very slender conical teeth along most of its length; there are 44 teeth on the right dentary in the single specimen we counted (UF 168246). At its anterior tip, the dentary curves sharply medially and is in the form of a prominent boss. The coronoid process of the dentary is high and is overlapped laterally by the upper jaw elements so that only the toothed portion of the dorsal margin of the dentary is visible in lateral view. The posterior portion of the lower jaw comprises the anguloarticular and the retroarticular; all three bones (i.e., the angular, articular, and retroarticular) are autogenous in the larval specimen examined here (USNM 388226). The pointed anterior end of the anguloarticular fits into a socket formed by the dentary. The articular surface of the lower jaw is positioned on the posteroventral corner of the anguloarticular and is a well-defined notch. The retroarticular, which is separated from the jaw joint, is almost entirely hidden in lateral view by the anguloarticular. The coronomeckelian is a small, irregularly shaped bone that straddles the contact point between Meckel's cartilage and the articular ossifications. The mandibular sensory canal is contained in both the dentary and anguloarticular; in the dentary it opens through a series of pores.

Ventral portion of the hyoid arch.—The ventral portion of the hyoid arch is well ossified and comprises a basihyal, dorsal and ventral hypohyals, anterior and posterior certatohyals, and an interhyal (Fig. 5A, B). The hypohyals contact one another medially and form a blunt anterior margin of the hyoid arch. The rectangular anterior ceratohyal bears a distinct "beryciform" foramen, which may or may not be completely closed dorsally. The anterior margin of this foramen also may bear a posteriorly directed process. The triangular posterior ceratohyal has a slightly concave articular surface for contact with the interhyal. The interhyal is broader ventrally, where it contacts the posterior ceratohyal, than at its dorsal contact with the suspensorium.

There are seven branchiostegals, four supported by the anterior ceratohyal, one by the cartilage between the two ceratohyals, and two by the posterior ceratohyal. The posterior four branchiostegals contact the lateral surface of the hyoid arch, whereas the anterior three attach to the ventral margin of the anterior ceratohyal, a pattern seen in all other carangids examined.
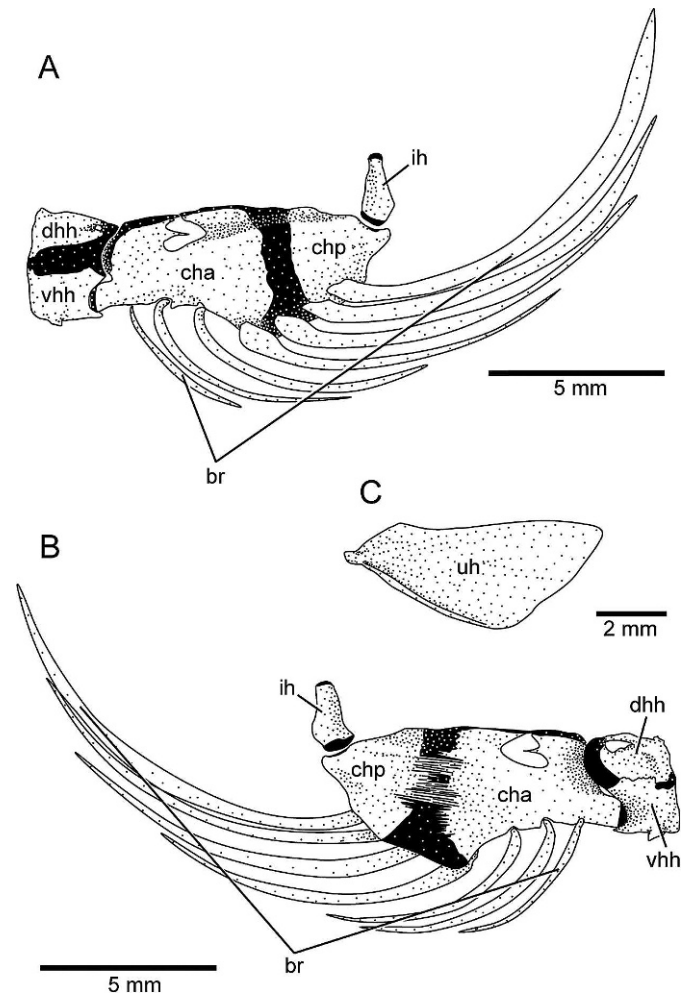

Fig. 5. Portions of the ventral hyoid arch of *Parastromateus niger* (ANSP 62088, 120 mm SL). (A) Lateral and (B) medial views of the ventral hyoid arch, with the exception of the basihyal (see Figs. 6, 7). (C) Urohyal in lateral view. Anterior facing left in (A, C); anterior facing right in (B). Bone in stipple, cartilage in black. Abbreviations: br, branchiostegal; cha, anterior ceratohyal; chp, posterior ceratohyal; dhh, dorsal hypohyal; ih, interhyal; uh, urohyal; vhh, ventral hypohyal.

The urohyal (Fig. 5C) is a roughly triangular element shaped like an inverted "T" in cross section. It is unusual among carangids in lacking a distinct dorsal ramus, although the anterior part of the dorsal margin rises slightly.

Gill arches.—The gill arches are distinctive among carangids, in part because of the greatly elongated teeth associated with all pharyngeal toothplates and gill rakers. The four epibranchials (eb1–4) are all differently shaped. Epibranchial 1 bears a well-developed uncinate process at about its midpoint (Fig. 6A). The uncinate process of eb1 is forked. The anterior arm of the uncinate process, which articulates with the interarcual cartilage, is closely aligned with the proximal end of eb1 (Fig. 6B). The first pharyngobranchial is vertically oriented, proximally contacting the prootic and distally contacting the junction between the proximal end of eb1 and a small cartilaginous medial division of eb1 (Fig. 6B), which is also found in many other carangid taxa. The medial end of eb2 is broad, with its cartilage tip contacting cartilaginous prominences of both pb2 and pb3. Epibranchials 3 and 4 are in close approximation in their midpoints, and nearly contact each other through cartilag-
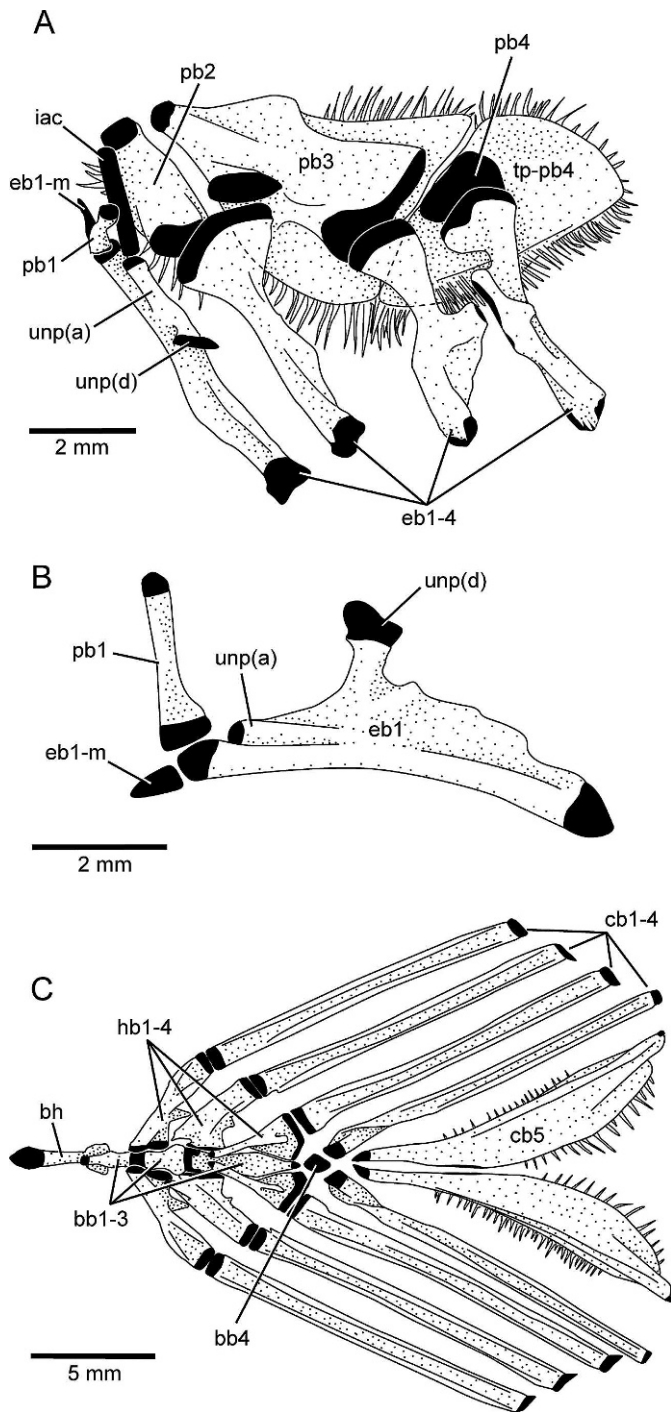
Fig. 6. Gill arches of *Parastromateus niger* (ANSP 62088, 120 mm SL). (A) Dorsal gill arches from left side in dorsal view. (B) Dorsal portions of first gill arch in anterolateral view. (C) Ventral gill arches in ventral view. Anterior facing left. Bone in stipple, cartilage in black. Gill rakers omitted. Abbreviations: bb, basibranchial; bh, basihyal; cb, ceratobranchial; eb, epibranchial; eb1-m, medial cartilaginous division of eb1; hb, hypobranchial; iac, interarcual cartilage; pb, pharyngobranchial; tp-pb4, tooth plate of pb4; unp(a), anterior fork of uncinate process of eb1; unp(d), dorsal fork of uncinate process of eb1.

inous regions of each element. The toothplates associated with pb2 and pb3 are fused to their respective gill arch elements, whereas that of pb4 remains separate from the cartilaginous pharyngobranchial. On the dorsal surface of pb3, there is a distinctly raised plateau, which articulates with eb3 and pb4. There is also a distinctive toothplate

formed by the fusion of gill rakers (separate in the larval specimen examined here), which bridges the eb4–ceratobranchial 4 (cb4) articulation (Fig. 7B, D).

The ventral portions of the gill arches consist of five paired ceratobranchials (cb1–5), three paired hypobranchials (hb1–3), and a series of median basibranchials—three ossified basibranchials in an anterior copula (bb1–3) and a posterior basibranchial copula that remains cartilaginous and represents basibranchial 4 (bb4). The basihyal and basibranchial elements lack toothplates. Most carangids have such toothplates (paired toothplates in *Scomberoides* and *Oligoplites*, median toothplates in *Parona*, and randomly scattered toothplates in most other genera; see Nelson, 1969 and Smith-Vaniz and Staiger, 1973). The absence of basibranchial and basihyal toothplates within the family Carangidae was only otherwise observed in *Hemicaranx*, *Trachinotus*, and *Uraspis*, among the taxa examined in the present study. The median basihyal is closely associated with the dorsal surface of bb1 (Figs. 6C, 7C). Ceratobranchials 1–4 are subequal in length and are elongate straight bars of bone with a ventral concave surface forming a trough for the branchial blood vessels. Ceratobranchial 5 differs by being slightly shorter and curved and much broader, particularly in its midsection, where, on its dorsal surface, it supports a large patch of teeth. This tooth patch extends for much of the length of cb5 and is formed by elongate, almost filamentous teeth of similar form as those of the dorsal tooth plates.

Vertebral column.—There are 10+14 vertebrae (Smith-Vaniz, 1984; Springer and Smith-Vaniz, 2008; pers. obs.). The neural spines of the first two vertebrae incline anteriorly, following the angle of the posterior margin of the supraoccipital crest (Figs. 2C, 7A, B). More posteriorly, the neural spines are elongate and nearly vertical but become progressively shorter and posteriorly inclined posteriorly in the caudal region (Fig. 8). The first neural arch is autogenous. There are well-developed neural zygapophyses on all vertebrae and haemal zygapophyses on the posteriormost few abdominal vertebrae and all caudal vertebrae. The haemal spines are well developed. The anteriormost haemal spine is slightly curved anteriorly, whereas the more posterior haemal spines mirror the neural spines and transition from a vertical orientation to become posteriorly inclined.

Inferior vertebral foramina are present on the vertebrae of the posterior abdominal region and most of the caudal region. The foramina on the abdominal vertebrae are positioned near the bases of the parapophyses and are much smaller than those on the caudal vertebrae, which pierce the bases of the haemal arches. The anteriormost vertebra with an inferior vertebral foramen varies from v4 to v8. Frequently, the anteriormost vertebra with a foramen has only a small, indistinct foramen on one or the other side of the vertebra (not visible on radiographs; Springer and Smith-Vaniz, 2008:fig. 8). All specimens have well-developed inferior vertebral foramina posterior to and including vertebra 8. Obvious inferior vertebral foramina are present on caudal vertebrae 1–11 in all specimens and at all stages (i.e., larval, juvenile, and adult), although they are smaller on the more posterior vertebrae than those anterior on the vertebral column, particularly in larger indivduals. Smith-Vaniz (1984:table 1) reported that within carangids, inferior vertebral foramina are restricted to Carangini and the trachinotin *Lichia*. Springer and Smith-Vaniz (2008) recently
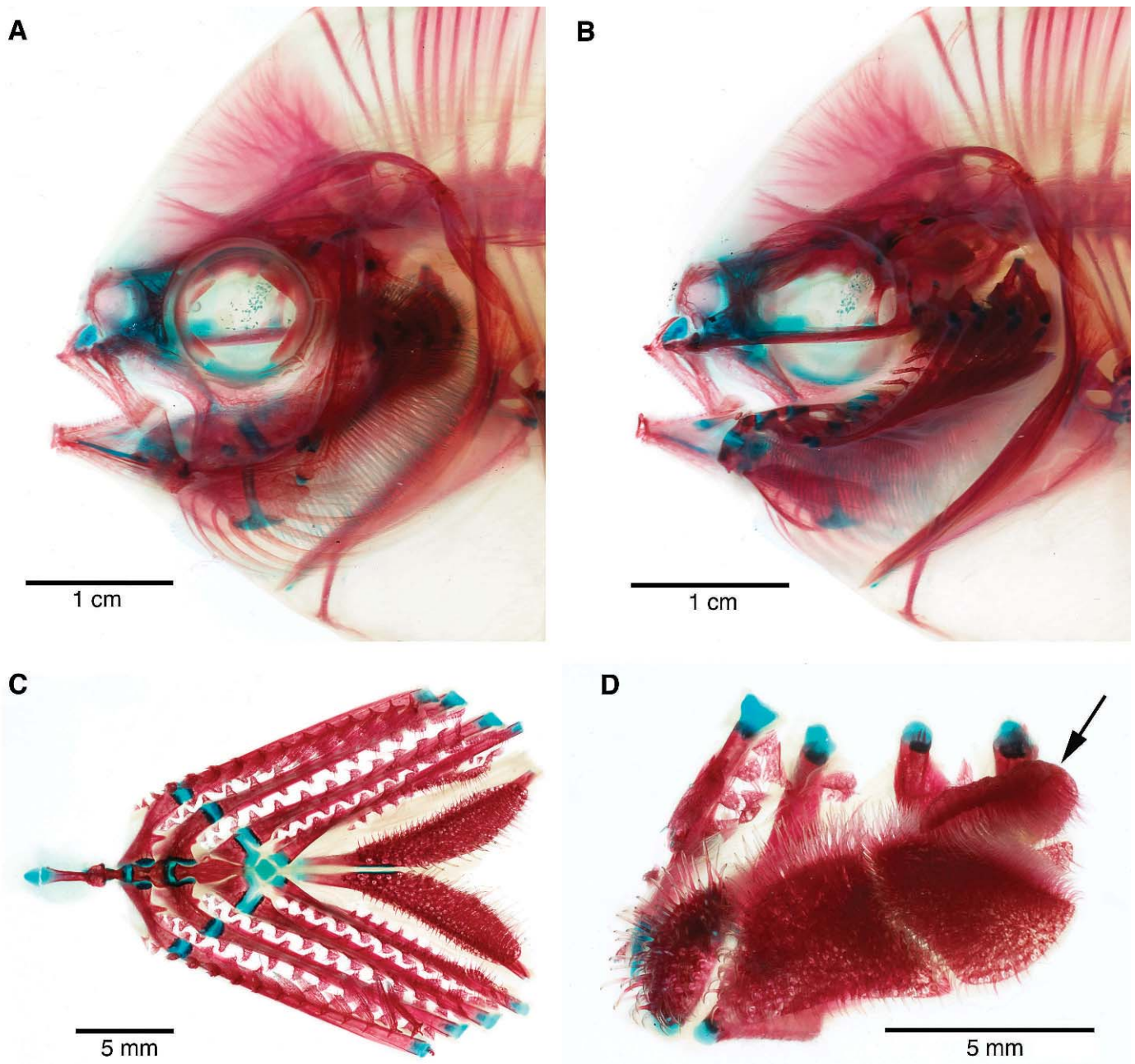
Fig. 7. Cleared-and-stained specimens of *Parastromateus niger* (ANSP 62088, 120 mm SL). (A) Lateral view of skull, intact. (B) Lateral view of skull with jaws, suspensorium, and infraorbital bones removed to show position of gill arches *in situ* (right side, image reversed). (C) Ventral gill arches in dorsal view. (D) Dorsal gill arches in ventral view; arrow indicates enlarged tooth plate positioned between the anterior and posterior rows of gill rakers and bridging the eb4–cb4 joint. Anterior facing left. Bone stained red, cartilage stained blue.

noted that specimens of *Parona* (Scomberoidini) less than 100 mm SL have these foramina, but that they are lost during later development.

Rudimentary parapophyses are present on the first two vertebrae but become longer and more pronounced posteriorly along the vertebral column beginning at the third vertebra. As is typical for teleosts (Patterson and Johnson, 1995), the ribs begin on the third vertebra. All ribs are elongate, gently curved elements except for the last pair, which are short, stick-like bones. The distal tips of the third- and second-to-last pairs of ribs extend posteriorly, contacting the first and second haemal spines. The series of epineural bones, which begin on the first vertebra, is largely confined to the abdominal region, although the epineural

ligaments of the first few caudal vertebrae may also be ossified.

Caudal fin and supports.—The skeletal support for the caudal fin is very similar to that reported for other carangins (Hollister, 1941; Monod, 1968; Fujita, 1990) and was illustrated previously by Witzell (1978:fig. 7). The caudal fin is supported by the axial skeletal elements posterior to and including pu3 (Fig. 9). The anterior dorsal and ventral procurrent fin rays (i.e., the unsegmented rays along the leading edges) are much thicker than the more-posterior fin rays and are not directly supported by skeletal elements, but rather lie in the intervertebral space between pu3 and pu4. There are 17 (9 dorsal + 8 ventral) principal caudal-fin rays
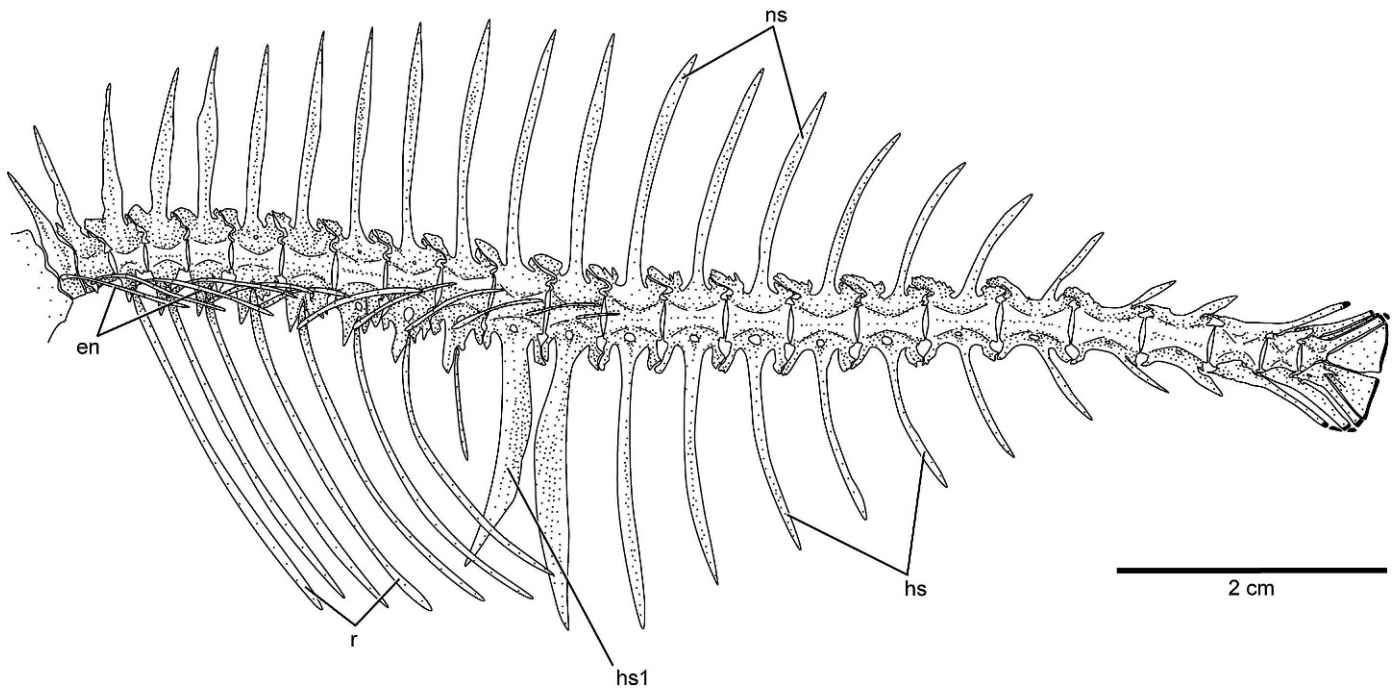
Fig. 8. Vertebrae of *Parastromateus niger* (ANSP 62088, 120 mm SL). Anterior facing left. Bone in stipple, cartilage in black. Abbreviations: en, epineural; hs, haemal spine; ns, neural spine; r, rib.

(branched fin rays plus the last dorsal and ventral unbranched fin rays). The caudal-fin rays are arranged so that dorsally and ventrally they deeply invest the endochondral elements of the caudal skeleton, but towards the fork of the fin (i.e., on either side of the diastema), they barely contact the hypurals.

In large juveniles and adults, the urostylar centrum and uroneural are fused, and this element supports the parhypural and hypural elements (Fig. 9B). The uroneural portion of this compound element tightly surrounds the proximal

and dorsal surfaces of hypural 5 forming a very rigid articulation; these elements become fused, as in other carangids (Hollister, 1941; Monod, 1968; Hilton and Johnson, 2007), by 120 mm SL. There are three hypural elements, representing hypurals 1+2, 3+4, and 5 (hypural 5 is fused to the urostylar centrum/uroneural compound element). In our smallest specimen (Fig. 9A), the compound hy1+2 and hy3+4 clearly show evidence of this fusion. There are three distal caudal radials (=post-hypural cartilage and post-haemal spine cartilages of Fujita, 1990) associated with
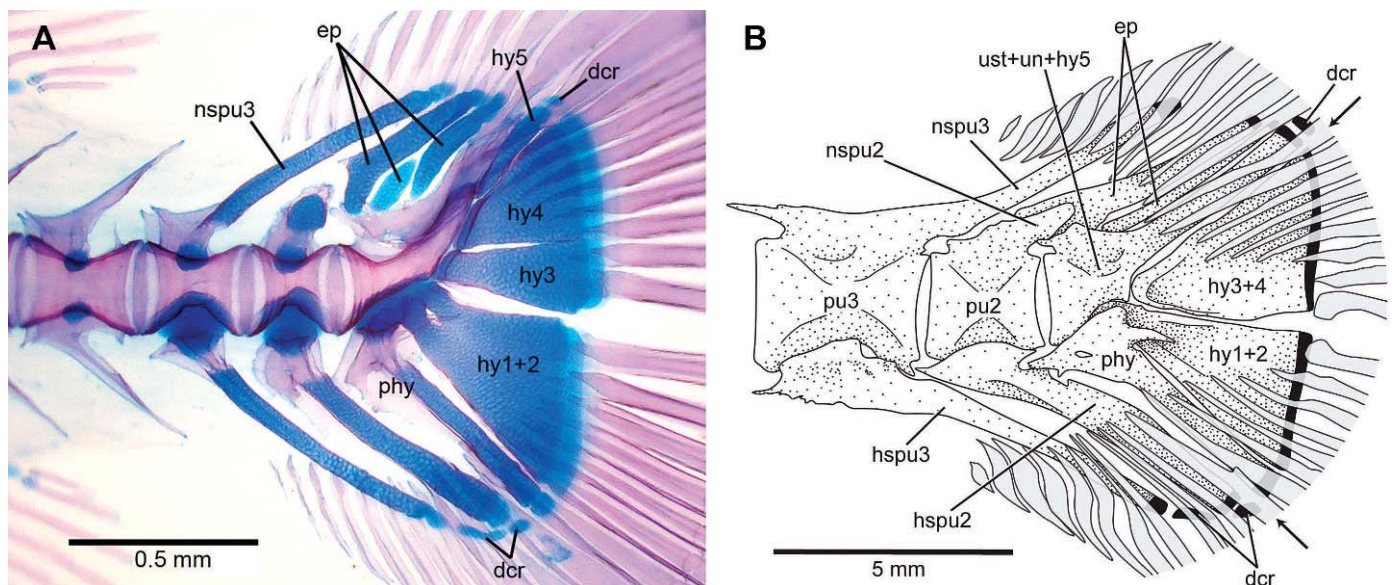

Fig. 9. Caudal skeleton of *Parastromateus niger*. (A) Photograph of cleared-and-stained larval specimen; bone stained red, cartilage stained blue (USNM 388226, 11 mm SL). (B) Line drawing of large juvenile specimen (ANSP 62088, 120 mm SL); bone in stipple, cartilage in black. Proximal portions of fin rays shown in light gray; arrows indicate the longest dorsal and ventral unbranched caudal-fin ray (=dorsalmost and ventralmost principal caudal-fin rays). Anterior facing left. Abbreviations: dcr, distal caudal radial; ep, epural; hspu, haemal spine of preural centrum; hy, hypural; nspu, neural spine of preural centrum; phy, parhypural; pu, preural centrum; un, uroneural; ust, urostylar centrum.

the haemal spine of preural 2 and 3, and hypural 5. The radial associated with hspu3 is the most elongate.

Similar to other carangids, the proximal ends of the epurals fit into grooves formed by the rudimentary neural spine of preural 2, and the uroneural portion of the compound uroneural + urostylar centrum. In our smallest individual, there are three epurals (Fig. 9A), whereas in larger specimens there are only two epurals (Fig. 9B). These epurals likely represent ep1 and ep3, although it is unknown if ep2 ossifies and fuses to ep1 (as in, for example, *Selene vomer*) or if it atrophies and eventually disappears (as in *Caranx crysos*); see Hilton and Johnson (2007) for discussion of the different ontogenetic pathways of the epurals in different carangins. Witzell (1978) also illustrated a small ep2 in *Parastromateus* (the size of the illustrated specimen was not reported).

Dorsal and anal fins and supports.—The dorsal-fin ray formula is IV–V+I, 41–44 and that of the anal fin is II+I, 35–39 (Smith-Vaniz, 1984). The leading fin spines of both fins are deeply embedded in the skin.

The first dorsal pterygiophore typically supports a single supernumerary spine followed by four spines serially associated with the first four pterygiophores (i.e., five spines supported by four pteryiophores; Fig. 10B). Occasionally there are two supernumerary spines associated with the first dorsal-fin pterygiophore, suggesting that this is the product of fusion of two distinct pterygiophores during the ontogeny of these individuals (Springer and Smith-Vaniz, 2008), as found in many perciforms (Fritzsche and Johnson, 1980).

The proximal-middle radials of both the dorsal and anal fins insert deeply into the interneural and interhaemal spaces, respectively. Posterior to the anteriormost interneural space to include pterygiophores (interneural space 2), there are between one and three pterygiophores per space (a single pterygiophore is an infrequent variant); interneural space 2 receives between two and four pterygiophores (Springer and Smith-Vaniz, 2008). In the anal fin, there are between two and four pterygiophores inserting between the haemal spines, with the exception of the anteriormost interhaemal space, which has between nine and 11 pterygiophores crowded into it (Fig. 10F; Springer and Smith-Vaniz, 2008). Springer and Smith-Vaniz (2008) found that *Parastromateus* is unusual among extant acanthomorphs in having more than eight pterygiophores in this space (a single larval specimen they cited, shown in Fig. 1C, and which they regarded as aberrant, has only seven). Springer and Smith-Vaniz (2008) provided comprehensive documentation and discussion of the pterygiophore insertion patterns in carangid fishes, including a detailed description of *Parastromateus*.

The proximal expansions of the fin rays completely embrace the distal radials. The distal radials are median structures, although each cartilage supports a pair of ossifications on its lateral surfaces that articulate with its associated fin ray (Fig. 10D, E). Although our observations on the development of the fins and their supports are limited, it appears that there is an anterior to posterior direction of ossification, as the anteriormost distal radials are well ossified and the posteriormost are entirely cartilaginous in our largest cleared-and-stained specimens (dry skeletons were not disarticulated). The largest anal-fin pterygiophore is the anteriormost of the series and is tightly associated with the anterior margin of the first haemal spine. This pterygiophore supports the anterior two (supernumerary) spines. The posteroventral corner of the first anal pterygiophore is protracted and overlaps the first distal radial, which is elongate and well ossified (i.e., it is not composed of two small ossifications); the third anal-fin spine is serially associated with this element.

Pectoral girdle and fin.—The pectoral fin comprises 20–23 fin rays. The leading fin ray is supported by the first distal radial, which is the largest of the series (and also supports the next anterior fin ray), and the scapula (Fig. 11C). The base of this fin ray has an elongate anterior extension that contacts the scapula. The remaining fin rays are each associated with a single cartilaginous distal radial, each of which decrease in size anterodorsally to posteroventrally. There are four ossified pectoral radials that are supported by the scapula (ra1–2) or the cartilaginous scapula–coracoid suture (ra3–4). The dorsalmost radial is the smallest and the fourth the longest; all have a constricted central region.

The chondral components of the pectoral girdle include the scapula and the coracoid, which contact one another in a broad cartilage-filled suture (i.e., the unossified portion of the scapulocoracoid cartilage). Anteriorly, this suture is highly interdigitating, but the margins of the two bones become smooth posteriorly. The scapula is a small, somewhat square bone that entirely encloses the scapular foramen (Fig. 11C). The coracoid, in contrast, is an elongate element that tapers to an anterior point. The anteroventral tips of the cleithrum and the coracoid from the left and right sides approach each other in the ventral midline of the body.

The dermal components of the pectoral girdle consist of the posttemporal, supracleithrum, cleithrum, and two postcleithra (Fig. 11A, B). Each posttemporal bears a prominent dorsal limb that articulates via its flattened ventral surface with the parietal–epioccipital crest of the skull roof. The ventral limb of the posttemporal, which articulates with the intercalar, is shorter and grades into the main body of the posttemporal. Both the posttemporal and the flattened supracleithrum carry portions of the trunk lateral line as it continues anteriorly into the cephalic sensory canal system from the lateral line scales. The cleithrum is the largest element of the pectoral girdle and has a strongly curved anterior margin delimiting its dorsal and ventral limbs, the main axes of which come together at an angle of approximately 120°. The short dorsal limb of the cleithrum (roughly corresponding to the portion that contacts the postcleithrum and supracleithrum) is sharply pointed dorsally. Laterally, the cleithrum supports a flange of bone that forms a groove that runs much of the length of the ventral limb of the cleithrum. The first postcleithrum is relatively broad and thin, particularly dorsoposteriorly where it grades out in the skin. The elongate second postcleithrum forms an angle of approximately 70° with the main axis of the ventral limb of the cleithrum, supporting the lateral regions of the abdominal cavity below the ribs. Ventrally, the second postcleithrum is protracted into a sharp point.

Pelvic girdle and fin.—In each pelvic fin, there is a short, sharply pointed spine and five pelvic-fin rays (Fig. 12A). Dorsally, the spine has a spherical articulation surface that contacts the pelvic bone, and ventrally bears a distinct
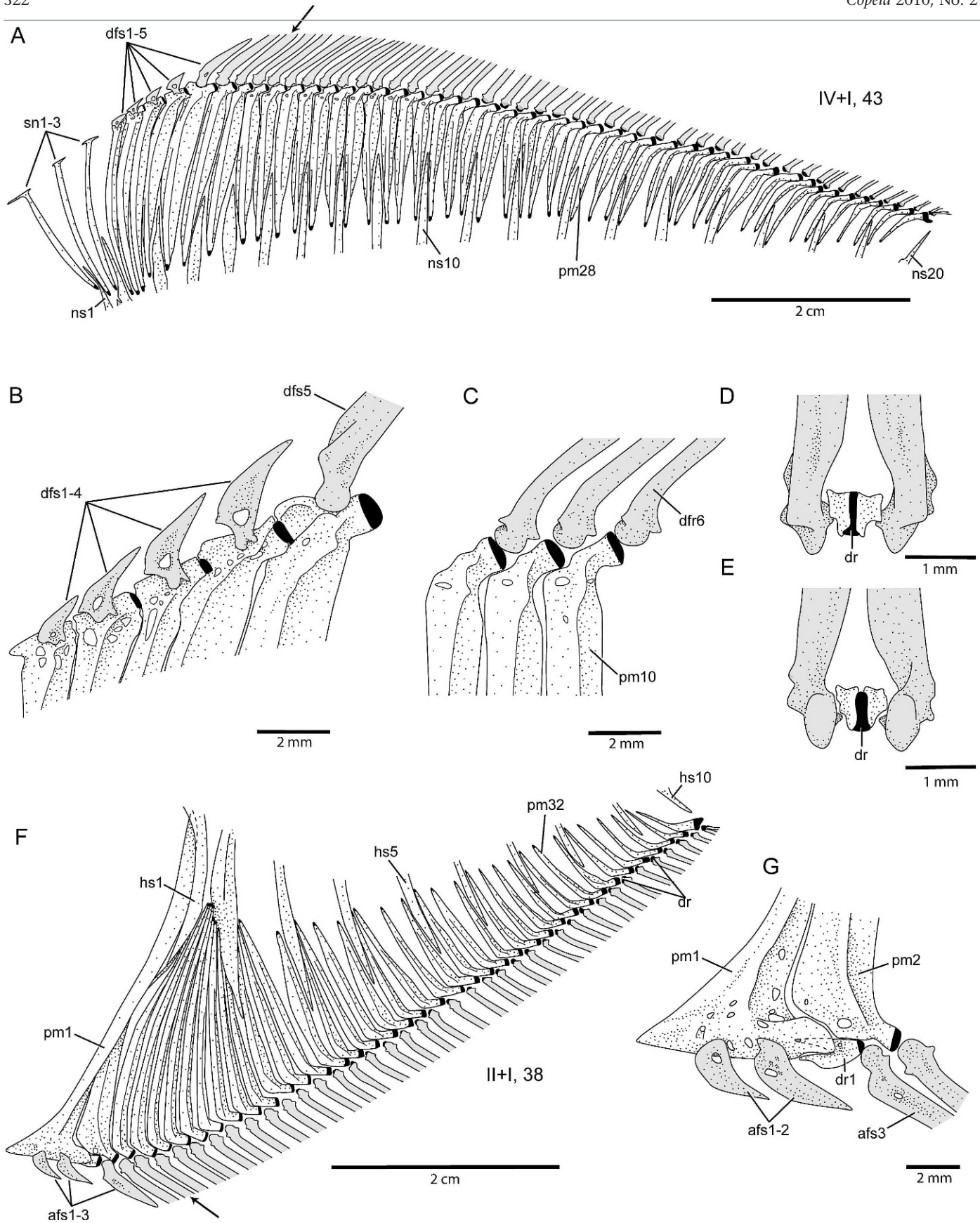
Fig. 10. Median fin supports of *Parastromateus niger* (ANSP 62088, 120 mm SL). (A) Supports of entire dorsal fin showing pattern of intercalation of proximal-middle radials and neural spines. Arrow indicates longest unbranched (=first principal) dorsal-fin ray. (B) Close-up of articulation of spines with proximal-middle radials. (C) Close-up of articulation of dorsal-fin rays and proximal-middle radials. (D, E) Articulation of dorsal-fin ray and distal radial in anterior (D) and posterior (E) views. (F) Supports of entire anal fin showing pattern of intercalation of proximal-middle radials and haemal spines. Arrow indicates longest unbranched (=first principal) anal-fin ray. (G) Close-up of articulation of anal-fin spines with proximal-middle radials. Anterior facing left in A–C, F, and G. Bone in stipple, cartilage in black, and proximal portions of fin rays shown in light gray. Abbreviations: afs, anal-fin spine; dfr, dorsal-fin ray; dfs, dorsal-fin spine; dr, distal radial; hs, haemal spine; ns, neural spine; pm, proximal-middle radial; sn, supraneural.
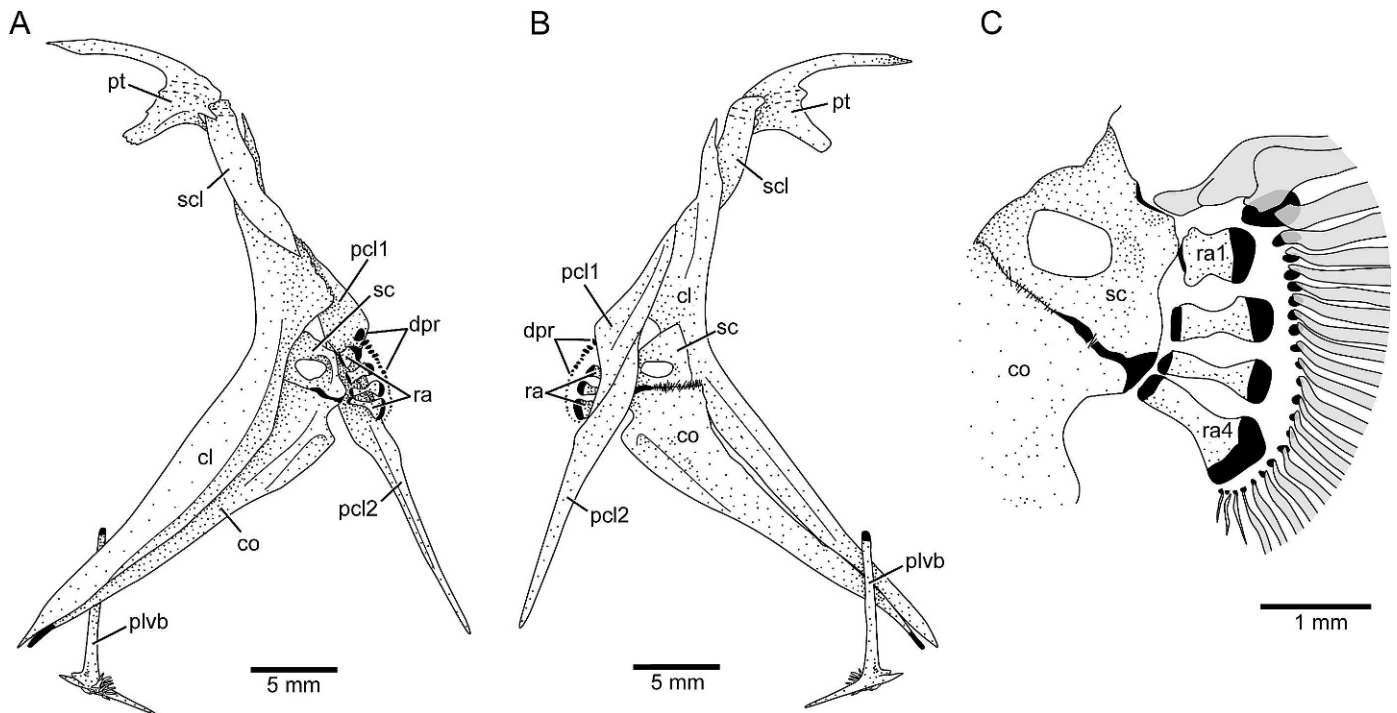
Fig. 11. Pectoral and pelvic girdles of *Parastromateus niger* (ANSP 62088, 120 mm SL). (A) Lateral view; anterior facing left. (B) Medial view; anterior facing right. (C) Detail of pectoral radials and fin rays; anterior facing left; proximal portions of fin rays shown in light gray. Bone in stipple, cartilage in black; dashed line indicates course of sensory canals. Abbreviations: cl, cleithrum; co, coracoid; dpr, distal pectoral radials; pcl, postcleithrum; plvb, pelvic bone; pt, posttemporal; ra, pectoral radials (=actinosts); sc, scapula; scl, supracleithrum.

pointed process that articulates with a hollow on the ventral surface of the pelvic bone. The first and second fin rays are the longest, and the remaining rays become increasingly shorter medially. Perhaps the most striking aspect of the pelvic fins is their reported ontogenetic loss at about 90 mm SL (Witzell, 1978). The timing of this loss is somewhat problematic in that the fin rays may be present but completely embedded in skin and not visible externally. For instance, in a 120 mm SL specimen (Fig. 12B), we

Fig. 12. Pelvic fin and girdle of *Parastromateus niger* in lateral view at two stages of development. (A) ANSP 150531 (73.6 mm SL). (B) ANSP 62088 (120 mm SL). Anterior facing left. Bone in stipple, cartilage in black; fin rays shown in light gray. Only left fin is shown and note that the hemilepidotrichia of each fin ray are disassociated from each other in B. Abbreviation: plvb, pelvic bone.

observed the rudiments of fin rays, although the components of each lepidotrichium have become disassociated from one another and do not reach the surface of the dermis. It is possible that such rudiments of the pelvic-fin rays are present in larger specimens but are overlooked or missing due to preparation as dried skeletons, although we found no trace of fin rays on a 132 mm SL alcohol-preserved specimen we dissected.

In contrast to the reduction and loss of fins, the pelvic girdle itself remains similarly shaped and well developed throughout ontogeny. The pelvic girdle consists of a pair of rod-shaped pelvic bones that are positioned between, and closely associated with, the medial surface of the antero-ventral portion of the pectoral girdle (Fig. 11A, B). There is an elongate, sharply pointed posteroventral extension of the pelvic bone and an anterolateral process that continues dorsally on the main shaft of the pelvic bone as a lateral crest (Fig. 12A), although the distinctiveness of this crest diminishes through ontogeny (Fig. 12B). Medially, the left and right pelvic bones contact one another through a short, Y-shaped process.
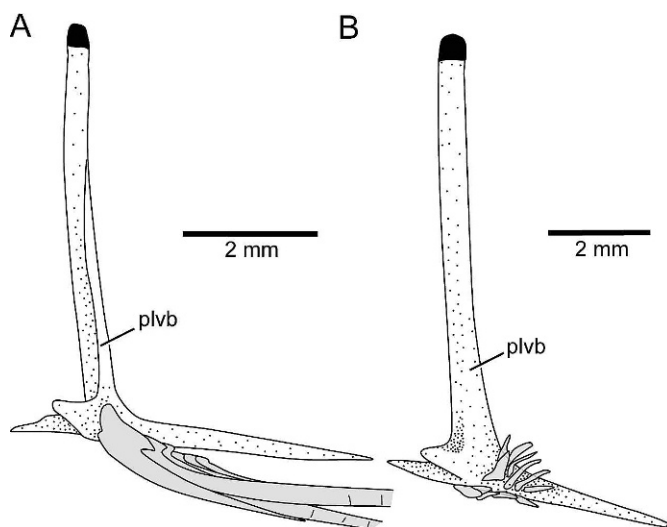
Scales and scutes.—The cycloid scales are small, rectangular, and numerous. In the single specimen (UF 168246) for which total lateral line scale/scute counts were obtained (counts from left and then right side recorded separately), there are 74/72 anterior scales and 15/13 scutes followed by 4/2 scales to the end of the hypural plate for a range of 87 to 93 total elements. This is in general agreement with de Beaufort and Chapman (1951), who reported about 100 "scales" along the lateral line. As in all carangins, scutes are present on the caudal peduncle of *Parastromateus*. There are between eight and 19 weakly developed scutes (Smith-Vaniz, 1986; Fig. 13), although the exact number is difficult
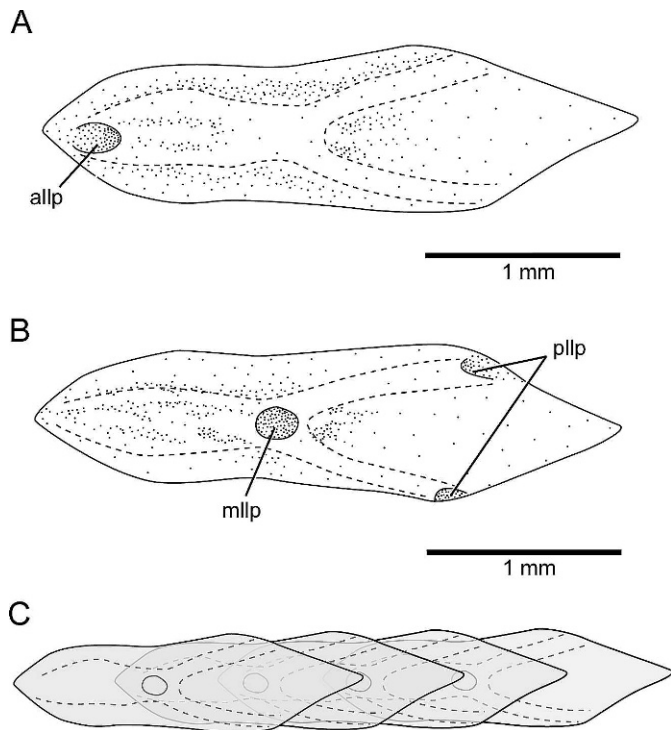
A

allp

1 mm

B

pllp

mllp

1 mm

C

Fig. 13. Scutes of *Parastromateus niger* (ANSP 62088, 120 mm SL). (A, B) Isolated scute from the middle of the series in external (A) and internal (B) views (image flipped). (C) Semi-schematic drawing of a series of four scutes showing the relationship of scutes with each other. The position of the external anterior pore of the lateral line canal has been omitted for clarity of the figure, but this opening receives the lateral line from the middle pore of the lateral line. Anterior facing left. Dashed line indicates course of the lateral line. Abbreviations: allp, anterior external lateral line pore of a scute; mllp, middle internal lateral line pore of scute; pllp, posterior external lateral line pores of scute.

to determine precisely because anteriorly the scutes grade smoothly into typical lateral line scales. All scutes are highly overlapping (Fig. 13C) and carry the lateral line sensory canal. Posteriorly on each scute the sensory canal is forked, with a dorsal and ventral branch (Fig. 13A, B), as in other carangins. Illustrations of a typical body scale and two lateral line scutes are also given by Yamada and Nakabo (1986).

DISCUSSION

***Taxonomy of* Parastromateus.**—Many different generic and specific names have been assigned to this taxon. Adults of *Parastromateus niger* have such a strong superficial resemblance to stromateids that Bloch (1795) assigned his new species to the genus *Stromateus*. Cuvier (in Cuvier and Valenciennes, 1832) recognized the unique taxonomic status of the species and described the new genus *Apolectus* for *Stromateus niger*; however, *Apolectus* is objectively invalid by homonymy, being preoccupied in fishes by *Apolectus* Bennett, 1831, a synonym of *Scomberomorus* Lacepède (Eschmeyer and Fricke, 2008). Whitley in McCulloch (1929), who was aware of Bennett's earlier name, proposed *Formio* as a replacement name. However, all three of these authors overlooked Bleeker (1864), who described *Parastromateus*, type species *Stromateus niger* Bloch 1795, by monotypy. Witzell (1978) gave a detailed synonymy in his important contribution to knowledge of the species, but
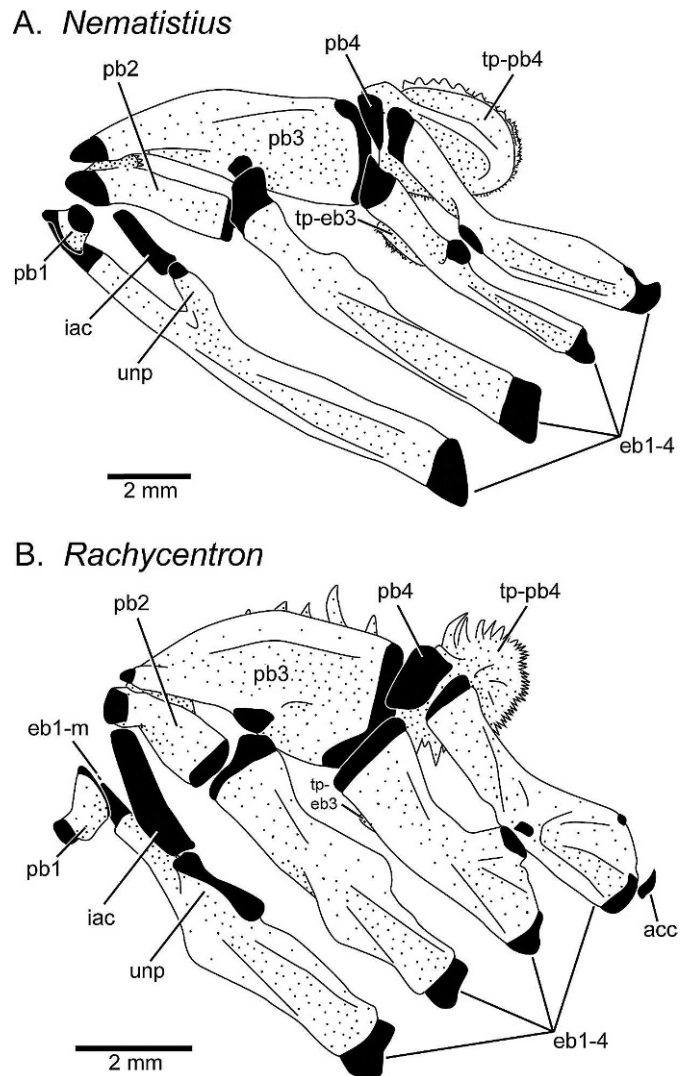
A. *Nematistius*

pb2

pb4

tp-pb4

pb3

tp-eb3

pb1

iac

unp

eb1-4

2 mm

B. *Rachycentron*

pb2

pb4

tp-pb4

pb3

eb1-m

tp-eb3

pb1

iac

unp

acc

eb1-4

2 mm

Fig. 14. Dorsal gill arches of selected non-carangid carangoids in dorsal view; from left side. (A) *Nematistius pectoralis* (ANSP 148654, est. 220 mm SL). (B) *Rachycentron canadum* (MCZ 157656, 157 mm SL). Anterior facing left. Bone in stipple, cartilage in black. Gill rakers and toothplate of eb2 omitted. Abbreviations: acc, accessory cartilage; eb, epibranchial; eb1-m, medial cartilaginous division of epibranchial 1; iac, interarcual cartilage; pb, pharyngobranchial; tp-eb3, toothplate of eb3; tp-pb4, tooth plate of pb4; unp, uncinate process of eb1.

continued to recognize *Apolectus* Cuvier 1832 as an available name. He erroneously believed that Cuvier's generic name predated Bennett's name. However, because *Apolectus* Cuvier 1832 applies to a different species (and family), according to rules of the International Code of Nomenclature (ICZN, 1999), it is unavailable for nomenclatural purposes.

Two species have been described based on juvenile specimens of *Parastromateus niger*. Richardson (1846) described *Seserinus vachelli* based on a juvenile from Canton, China Seas. Finally, Nichols (1950) described *Hildebrandella* for *Citula halli* Evermann and Seal, 1907 (also by monotypy) based on a juvenile from the Philippines.

Most authors prior to the 1900s had consistently classified *Parastromeus niger* and its various synonyms in the Stromateidae. Regan (1902) revised the Stromateidae and reassigned the species to the Carangidae. Jordan (1923) proposed the new family Apolectidae for *P. niger*, which
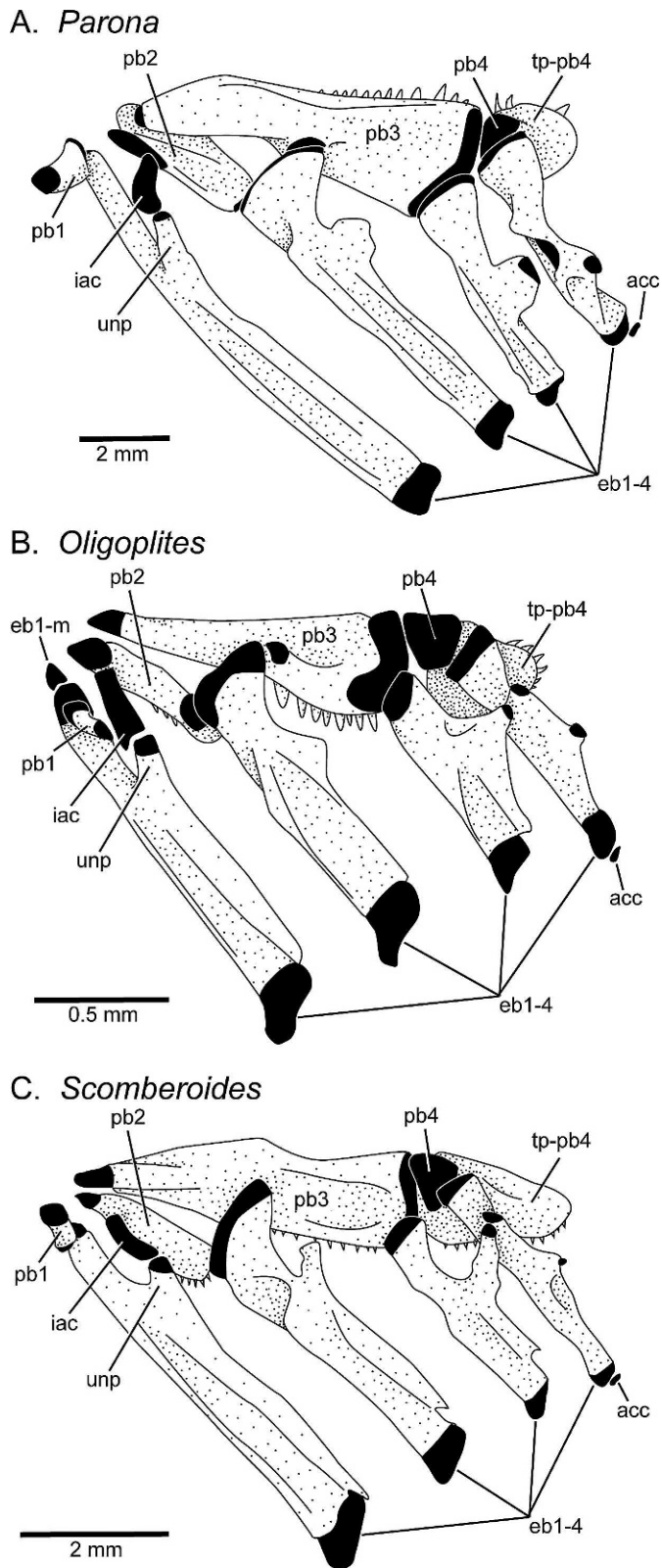
Fig. 15. Dorsal gill arches of Scomberoidini in dorsal view; from left side. (A) *Parona signata* (ANSP 148655, 184 mm SL). (B) *Oligoplites saurus* (USNM 383079, 37 mm SL). (C) *Scomberoides tala* (USNM 36080, 135 mm SL). Anterior facing left. Bone in stipple, cartilage in black. Gill rakers and toothplate of eb2 omitted. Abbreviations: acc, accessory cartilage; eb, epibranchial; eb1-m, medial cartilaginous division of eb1; iac, interarcual cartilage; pb, pharyngobranchial; tp-eb3, toothplate of eb3; tp-pb4, tooth plate of pb4; unp, uncinate process of eb1.
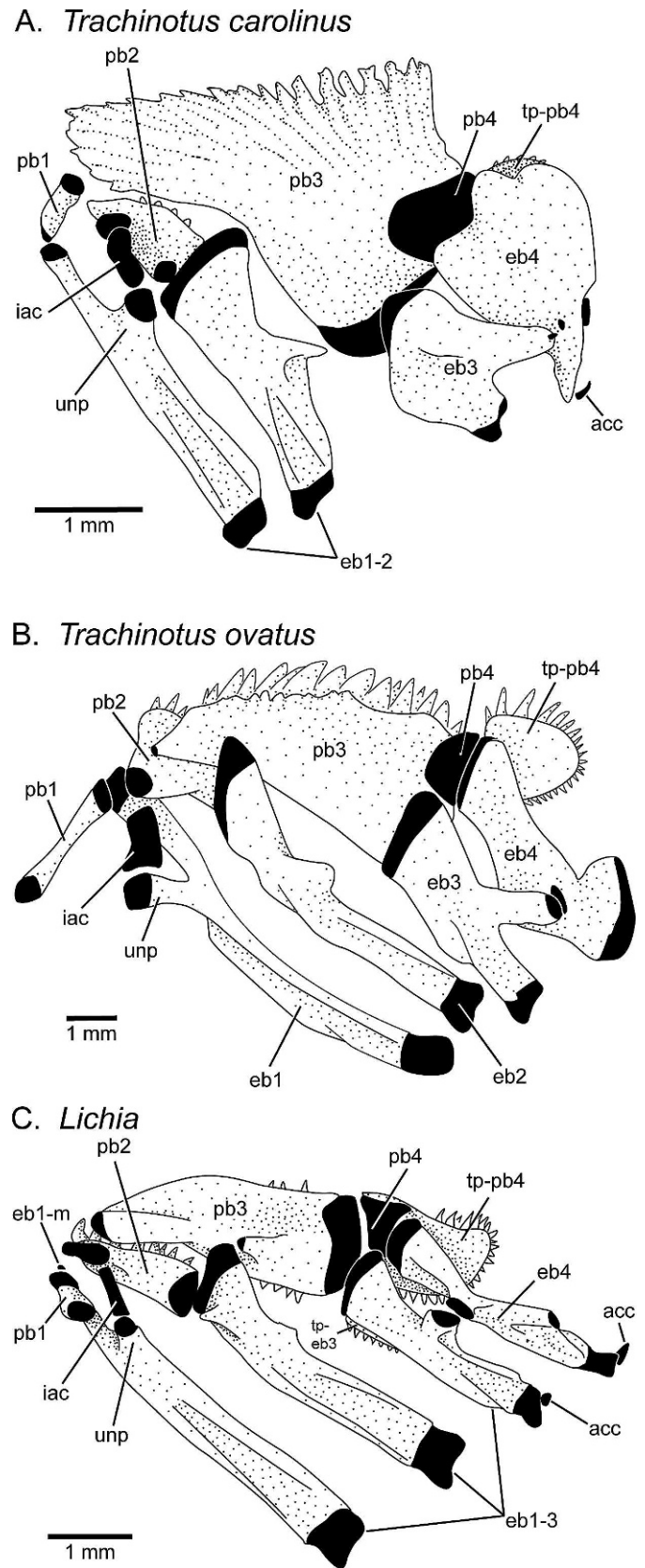

Fig. 16. Dorsal gill arches of Trachinotini in dorsal view; from left side. (A) *Trachinotus carolinus* (USNM 383083, 51 mm SL). (B) *Trachinotus ovatus* (USNM 319754, 70 mm SL). (C) *Lichia amia* (USNM 383085, 78 mm SL). Anterior facing left. Bone in stipple, cartilage in black. Gill rakers and toothplate of eb2 omitted. Abbreviations: acc, accessory cartilage; eb, epibranchial; eb1-m, medial cartilaginous division of eb1; iac, interarcual cartilage; pb, pharyngobranchial; tp-eb3, toothplate of eb3; tp-pb4, tooth plate of pb4; unp, uncinate process of eb1.
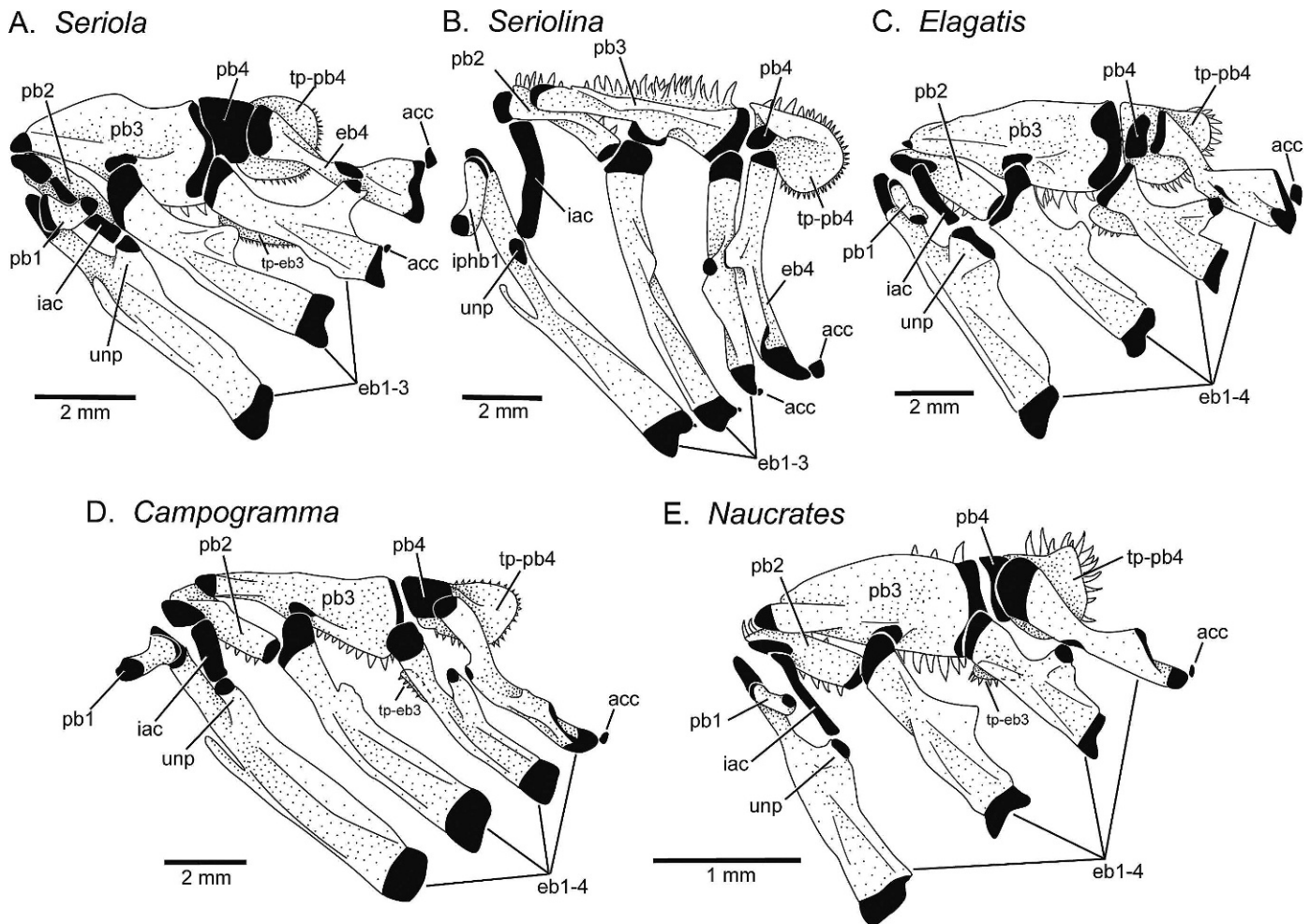
Fig. 17. Dorsal gill arches of Naucratini in dorsal view; from left side. (A) *Seriola fasciata* (MCZ 157674, 109 mm SL). (B) *Seriolina nigrofasciata* (ANSP 140622, est. 132 mm SL); note that tp-eb3 is present but is hidden in this view. (C) *Elagatis bipinulata* (MCZ 163480, 79 mm SL). (D) *Campogramma glaycos* (ANSP 135406, 166 mm SL). (E) *Naucrates ductor* (MCZ 164201, 37 mm SL). Anterior facing left. Bone in stipple, cartilage in black. Gill rakers and toothplate of eb2 omitted. Abbreviations: acc, accessory cartilage; eb, epibranchial; eb1-m, medial cartilaginous division of eb1; iac, interarcual cartilage; pb, pharyngobranchial; tp-eb3, toothplate of eb3; tp-pb4, tooth plate of pb4; unp, uncinate process of eb1.

Smith (1965) also adopted. Unaware of Jordan's Apolectidae, McCulloch (1929), on authority of Whitley, assigned the same species to the new family Formiidae (emended spelling Formionidae). Suzuki (1962), in his major study of the osteology of carangid fishes of Japan, excluded *Parastromateus* from the Carangidae, placing it in the family Formiidae. Without discussion, Greenwood et al. (1966), in their provisional classification of teleostean fishes, recognized the Formionidae as valid, listing Formiidae and Apolectidae as synonyms. Based solely on the lateral line canal system, Deng and Zhan (1986) also recognized a monotypic Formionidae. Apsangikar (1953) concluded that the phylogenetic position of *P. niger* justified classifying it in the new subfamily Parastromateinae with all other carangids assigned to the Caranginae. Most recent authors have followed Smith-Vaniz (1984) and Yamada and Nakabo (1986) in their firm placement of *Parastromateus* within the Carangidae. The only major exceptions are Witzell (1978) and studies of fossil fishes (Bannikov, 1987, 1990; Bannikov and Fedotov, 1984), where the Apolectidae is recognized as a valid family. The recognition of *P. niger* as the only extant member of a family would render the Carangidae paraphyletic unless all tribes (*sensu* Smith-Vaniz, 1984) and, following the phylogenetic position proposed by

Gushiken (1988), the group containing all carangins except *P. niger* were also elevated to families. Such proliferation of family-level names is not warranted.

Comparative anatomy of the dorsal gill-arch skeleton of carangid fishes.—As noted in the introduction, this study had its inception as a survey of the gill-arch skeleton of carangid fishes. Because some of the characters that we discovered may have phylogenetic significance and relevance to the affinities of *Parastromateus*, we present illustrations and brief comparisons of the dorsal gill-arch skeleton of carangid fishes generally; however, further comparative study of the gill arches in these fishes, including the musculature and the skeleton of ventral portions, is warranted. We emphasize here that for several of the 15 non-monotypic genera discussed below we have not examined the gill arches of the type species and in most cases have studied only one or two species of these genera. This is important, as additional nominal genera may ultimately be shown to be valid.

The basic structure of the dorsal gill-arch skeleton is relatively conserved across carangoids and comprises four epibranchials, four pharyngobranchials, associated tooth-plates (on pb2–4), an interarcual cartilage linking the
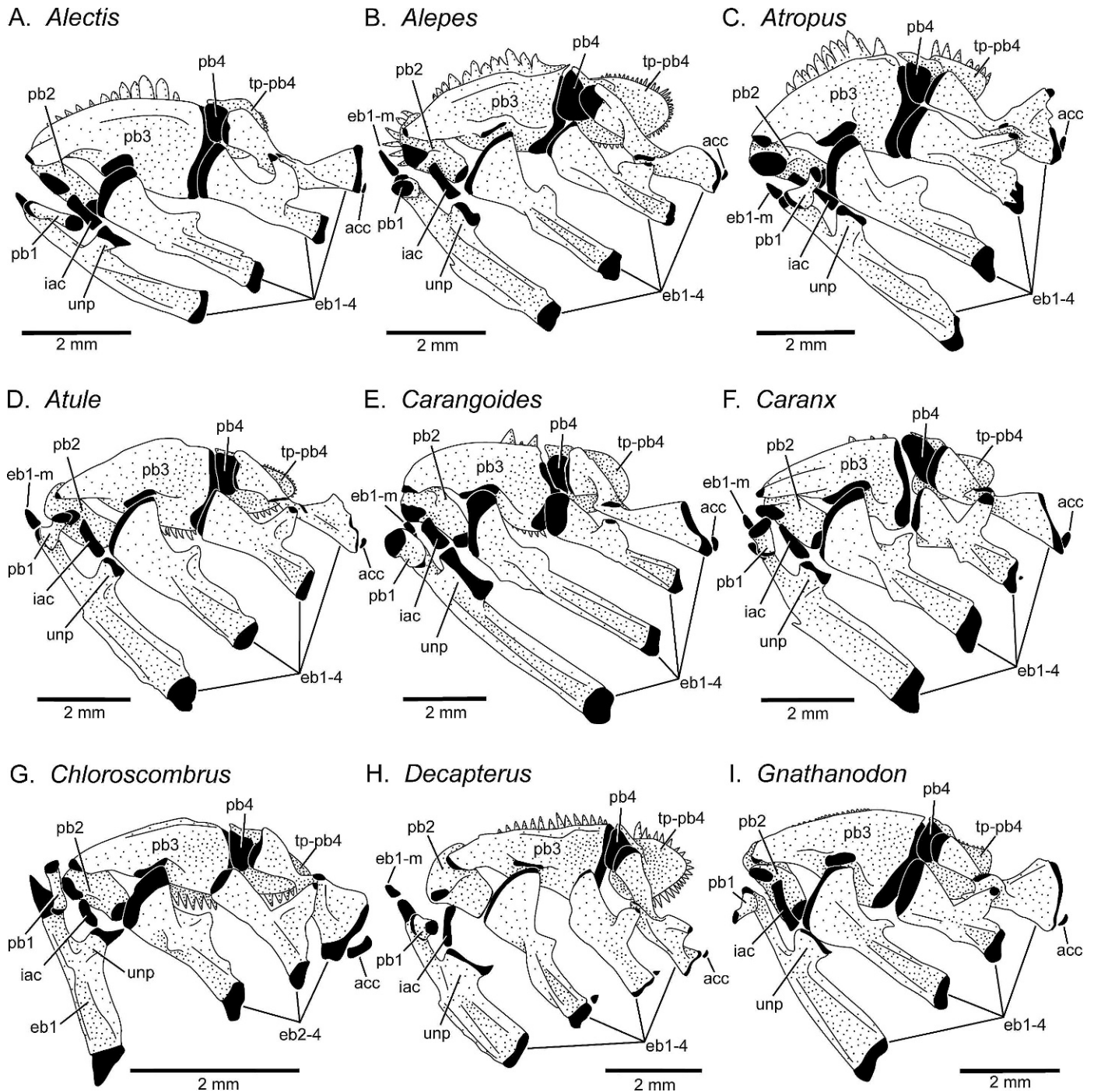
Fig. 18. Dorsal gill arches of Carangini in dorsal view; from left side unless otherwise noted. (A) *Alectis alexandrinus* (USNM 383089, 92 mm SL). (B) *Alepes djedaba* (USNM 347148, 110 mm SL); right gill arches, image reversed. (C) *Atropus atropos* (ANSP 144403, 95 mm SL). (D) *Atule mate* (USNM 325271, 110 mm SL). (E) *Carangoides plagiotaenia* (USNM 362714, 129 mm SL). (F) *Caranx crysos* (USNM 158866, 98 mm SL). (G) *Chloroscombrus chrysurus* (USNM 383077, 64 mm SL). (H) *Decapterus punctatus* (USNM 383086, 108 mm SL). (I) *Gnathanodon speciosus* (USNM 383087, 87 mm SL). Anterior facing left. Bone in stipple, cartilage in black. Gill rakers and toothplate of eb2 omitted. Abbreviations: acc, accessory cartilage; eb, epibranchial; eb1-m, medial cartilaginous division of eb1; iac, interarcual cartilage; pb, pharyngobranchial; tp-eb3, toothplate of eb3; tp-pb4, tooth plate of pb4; unp, uncinate process of eb1.

uncinate process of eb1 and the proximal head of pb2 (absent in *Echeneis*); accessory cartilages associated with the proximal end of eb1 and the eb4–cb4 joint are variably present (see below). *Pseudocaranx* is unique in having a dorsal extension of the anterior cartilaginous portion of pb2 (Fig. 19E; note that this extension appears posteriorly directed due to the orientation of pb2 in the figure).

In most carangids, the articulation between pb1 and the main body of eb1 (vs. the median accessory cartilage of eb1, which may lie medial to this articulation; see below) is flush and forms roughly a right angle, with the distal tip of pb1 lying dorsal to the proximal tip of eb1. In *Nematistius* and *Rachycentron* (but not *Coryphaena* or *Echeneis*), the distal tip of pb1 extends ventrally to become positioned medial to the proximal tip of eb1; a similar condition is also found in
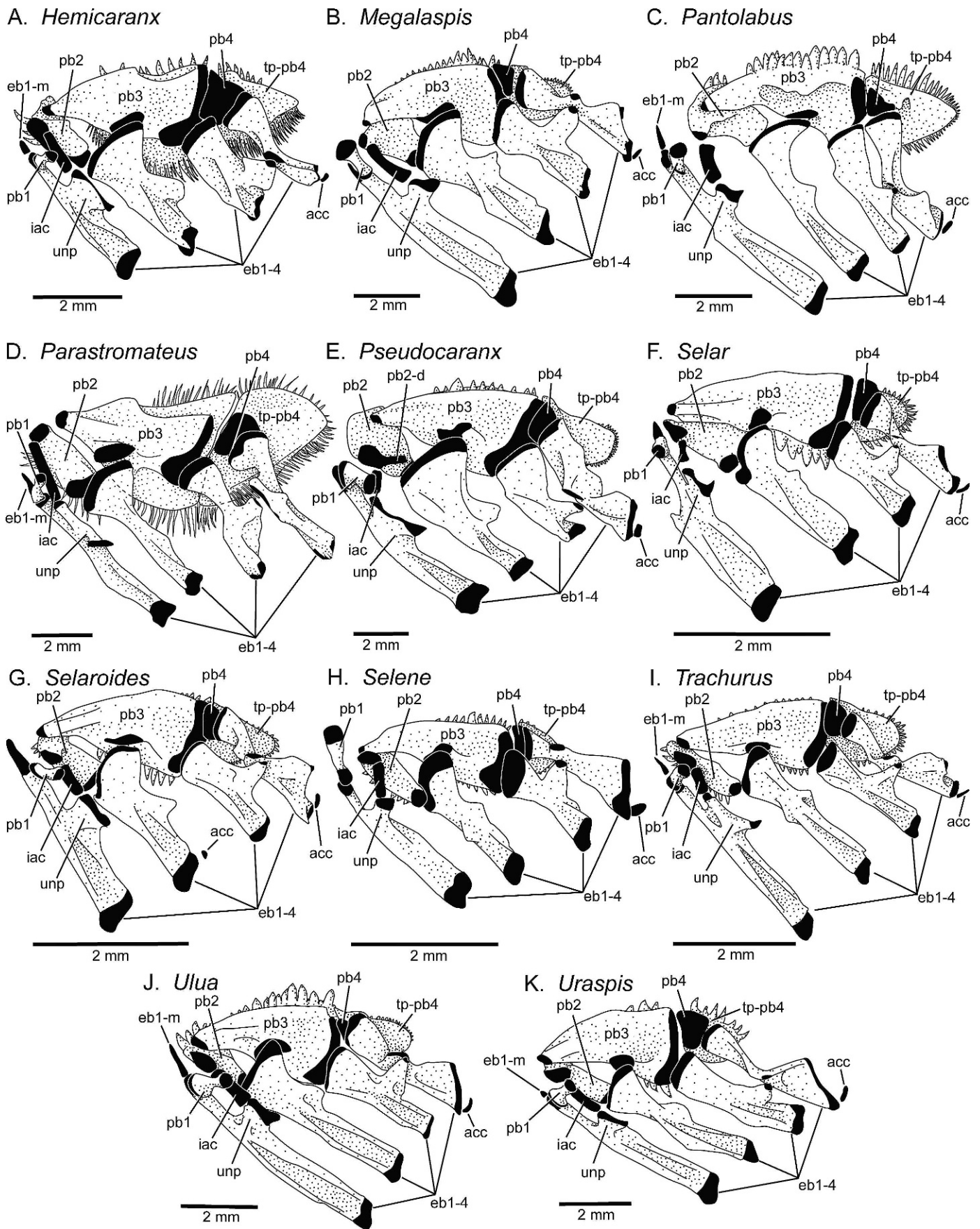
Fig. 19. Dorsal gill arches of Carangini in dorsal view; from left side unless otherwise noted. (A) *Hemicaranx amblyrhynchus* (ANSP 139101a, 106 mm SL). (B) *Megalaspis cordyla* (USNM 347146, 130 mm SL). (C) *Pantolabus radiatus* (ANSP 147709, 122 mm SL). (D) *Parastromateus niger* (ANSP 62088, 120 mm SL). (E) *Pseudocaranx dentex* (USNM 222104, 127 mm SL). (F) *Selar crumenophthalmus* (MCZ 149687, 56 mm SL). (G) *Selaroides leptolepis* (MCZ 59266, 65 mm SL); right gill arches, image flipped. (H) *Selene vomer* (USNM 383081, 54 mm SL). (I) *Trachurus*
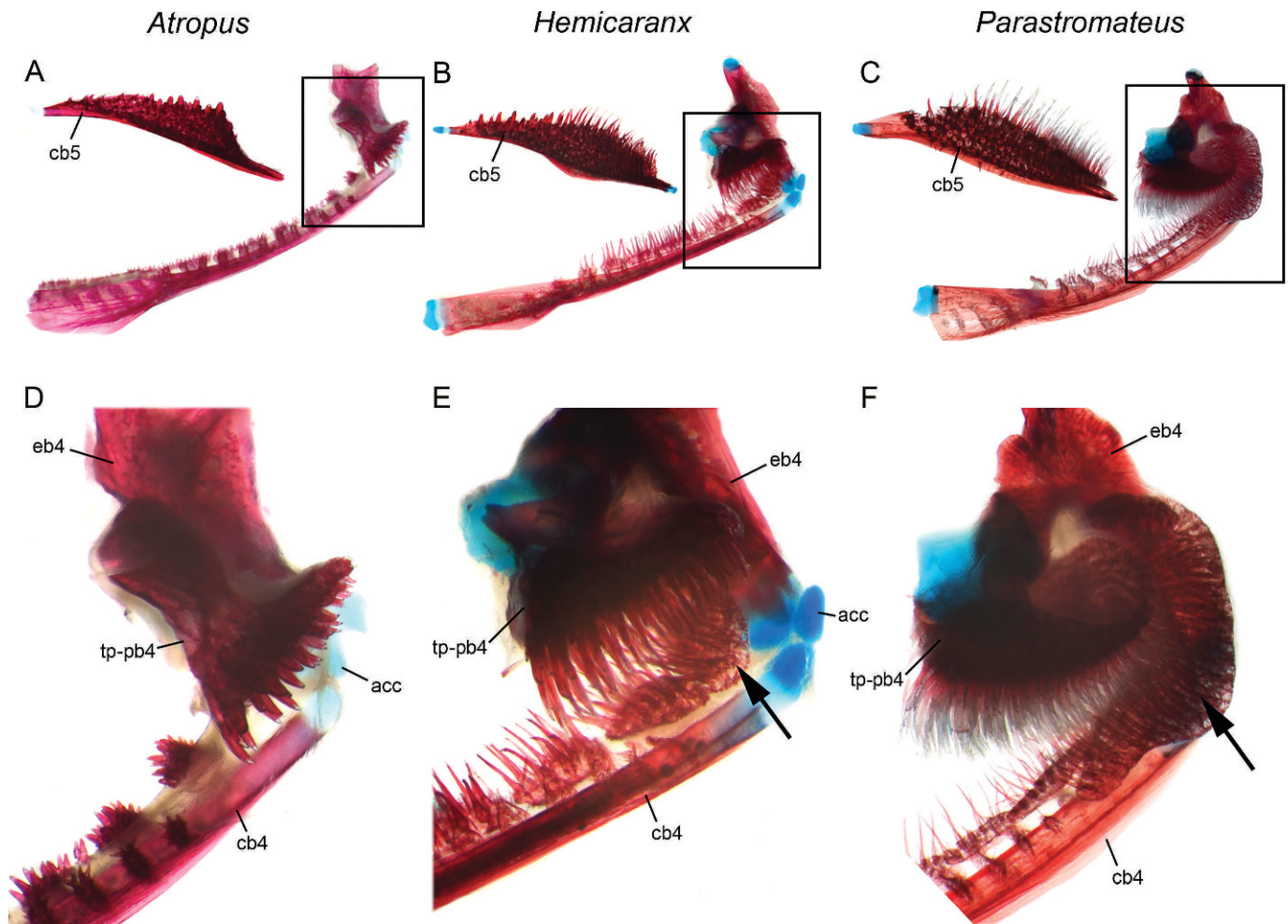
Atropus Hemicaranx Parastromateus

Fig. 20. Left cb5 in dorsal view showing the pharyngeal dentition and elements of the left fourth branchial arch in medial view (images reversed) showing the toothplate bridging the eb4–cb4 joint in *Hemicaranx* and *Parastromateus*. (A) *Atropus atropos* (ANSP 159005, 91 mm SL). (B) *Hemicaranx amblyrhynchus* (ANSP 139101, 85 mm SL). (C) *Parastromateus niger* (ANSP 62088, 100 mm SL). Boxes indicate area shown in close-up photos in D–F. Close-up photos showing elements of the left fourth branchial arch in medial view (images reversed) in (D) *Atropus*, (E) *Hemicaranx*, and (F) *Parastromateus*. Anterior facing left. Bone stained red, cartilage stained blue. Arrows indicate eb4–cb4 toothplate in *Hemicaranx* and *Parastromateus*. Abbreviations: acc, accessory cartilage; cb, ceratobranchial; eb, epibranchial; tp-pb4, toothplate of pb4.

Scomberoides (not visible in Figs. 14, 15C due to orientation of bones). In *Naucrates*, the proximal tip of eb1 is drawn out medially, so that it is far medial to the pb1–eb1 articulation. In Carangini, a similar condition is found in *Alectis*, *Chloroscombrus*, *Decapterus*, *Selar*, and *Selaroides*.

In all carangids, each epibranchial bears an uncinate process; those of eb1, eb3, and eb4 are cartilage tipped whereas that of eb2 is bony. The uncinate process of eb1 is variable in its form. It is markedly broad in some taxa (*Hemicaranx*, *Pseudocaranx*). In *Parastromateus*, it is bifurcate, with two cartilage-tipped processes, one short and dorsally directed, the other elongate and anteriorly directed; the anteriorly directed one articulates with the interarcual cartilage (Fig. 19D). A bifurcate uncinate process is otherwise found only in some species of *Trachurus* (Fig. 19I), where it is not as well developed as that of *Parastromateus*.

Within carangins, the cartilaginous tip of the uncinate process is drawn out into a point posteriorly in *Alectis*, *Alepes*, *Carangoides*, *Caranx*, *Chloroscombrus*, *Decapterus*, *Gnathanodon*, *Hemicaranx*, *Megalaspis*, *Pantolabus*, *Parastromateus*, *Pseudocaranx*, *Selar*, *Trachurus*, *Ulua*, and *Uraspis* (Figs. 18, 19).

We found a median accessory cartilage associated with the proximal tip of eb1 in many carangids. Among Carangini, a median accessory cartilage on eb1 is present in *Alepes*, *Atropus*, *Atule*, *Carangoides*, *Caranx*, *Decapterus*, *Hemicaranx*, *Pantolabus*, *Parastromateus*, *Selaroides* (although the specimen illustrated in Fig. 19G had the accessory cartilage only on the left side), *Trachurus*, *Ulua*, and *Uraspis* (Figs. 18, 19). This cartilage varies in size and shape ranging from small (e.g., in *Lichia*) to very elongate (e.g., *Alepes*), and it supports the dorsalmost portion of the anterior series of gill rakers. It is absent in all Naucratini, all scomberoidins except

mediterraneus (USNM 383084, 81 mm SL). (J) *Ulua mentalis* (USNM 347149, 100 mm SL). (K) *Uraspis* sp. (USNM 362716, 100 mm SL); right gill arches, image flipped. Anterior facing left. Bone in stipple, cartilage in black. Gill rakers and toothplate of eb2 omitted. Abbreviations: acc, accessory cartilage; eb, epibranchial; eb1-m, medial cartilaginous division of eb1; iac, interarcual cartilage; pb, pharyngobranchial; pb2-d, dorsal extension of pb2; tp-eb3, toothplate of eb3; tp-pb4, tooth plate of pb4; unp, uncinate process of eb1.

Oligoplites, and the trachinotin *Trachinotus* (Figs. 15, 16, 17). A very small median accessory cartilage was found in our specimen of *Rachycentron*, but is absent in *Nematistius*, *Coryphaena*, and *Echeneis*.

Most carangoids also have an accessory cartilage associated with the distal tips of cb4 and eb4 (henceforth ac4; see Springer and Johnson, 2004 for a description and discussion cb–eb accessory cartilages). Although Springer and Johnson (2004) reported finding ac4 in *Nematistius*, it is absent in our specimen (Fig. 14). *Parastromateus* appears to be unique among the Carangidae in lacking ac4 and an accessory cartilage associated with any other cb–eb joint. We found accessory cartilages associated with arches anterior to the fourth arch in several taxa (second arch in *Selaroides*, third arch in *Caranx*, *Lichia*, and *Seriola*, second and third arches in *Decapterus*, and all arches in *Seriolina*; Figs. 17, 18). Springer and Johnson (2004) found the presence of accessory cartilages in *Decapterus* to be individually variable.

All carangids examined have an enlarged autogenous toothplate associated with the proximal end of eb2 (not illustrated) that lies in series with the toothplate of pb2. Some carangoids have an enlarged gill raker that forms a toothplate associated with eb3, lying lateral to the toothplate of pb3. When present, this toothplate is usually fused to eb3 (in all taxa examined except *Coryphaena* and the naucratins *Naucrates* and *Campogramma*, in which it is autogenous). The toothplate of eb3 is absent in all Scomberoidini (*Parona*, *Oligoplites*, and *Scomberoides*), the trachinotin *Trachinotus* (which has greatly modified branchial arches utilized for durophagy; Grubich, 2003), and all Carangini examined. In *Parastromateus* and *Hemicaranx*, an enlarged toothplate bridges the eb4–cb4 joint (Fig. 20). This toothplate, which is unique to these genera among all carangids studied, develops from the fusion of gill rakers. As noted above, the teeth on the pharyngeal tooth plates of most carangid fishes are stout and conical (e.g., *Atropus*, Fig. 20A, D). In *Parastromateus*, however, these teeth are greatly elongated and filamentous (Fig. 20C, F); a similar condition is found in *Hemicaranx* (Fig. 20B, E).

***Systematic affinities of* Parastromateus.**—Witzell (1978) noted that *Parastromateus* shares several characters with certain carangids (e.g., protractile premaxillae, protruding lower jaw, a keeled lateral line, pharyngeal teeth, 10+14 vertebrae, inferior vertebral foramina on the caudal vertebrae, and first anal-fin pterygiophore lining the posterior margin of the abdominal cavity), but he concluded that it should be retained in its own family (Apolectidae) of unknown affinity because of its highly derived anatomy (although in the context of his study, the polarity of these characters was impossible to determine). The presence of the synapomorphies for the Carangoidei, including the presence of a prenasal canal bone and small adherent cycloid scales, allow *Parastromateus* to be firmly included in this group (Johnson, 1984; Smith-Vaniz, 1984). Further, Smith-Vaniz (1984) confirmed that *Parastromateus* is a member of the family Carangidae, citing the distinct separation between the second and third anal-fin spine, a synapomorphy of the family otherwise found only (slightly developed) in *Pomatomus* (Laroche et al., 1984). Smith-Vaniz (1984) further concluded that *Parastromateus* is a member of the tribe Carangini based, in part, on the presence of scutes.

In his cladistic analysis, Gushiken (1988) concluded that *Parastromateus* is the sister group of all other carangin genera

based on the presence of the two carangin synapomorphies (scutes along lateral line and inferior vertebral foramina [foramina were considered present otherwise only in *Lichia*]) and the absence of two characters defining all other carangins (pharyngeal teeth not uniformly villiform, and development of a subocular process on the subocular shelf). As shown in our study, at least one of these characters (the subocular process) is present in *Parastromateus*, and we consider the uniform nature of the pharyngeal teeth in this genus to be autapomorphic. Springer and Smith-Vaniz (2008) presented evidence from the post-cranial skeleton (e.g., insertion patterns of anterior pterygiophores of the anal fin; absence of pelvic fin in adults) that is suggestive of an affinity between *Parastromateus* and †*Paratrachinotus* from the Monte Bolca formation (Eocene, Italy). No other systematic analysis of carangid fishes, morphological or molecular (Reed et al., 2002), has addressed the position of *Parastromateus* within the family.

In our study of the dorsal gill arches of carangids, we discovered an enlarged toothplate that bridges the gap between eb4 and cb4 in *Parastromateus*, which we found elsewhere only in *Hemicaranx*. This toothplate is derived within a carangid framework and may be indicative of a sister-group relationship. These two genera also share elongate and filamentous pharyngeal dentition that is unlike that found in all other carangids. These genera also share single rows of very small conical teeth in both upper and lower jaws, and relatively small mouths with short upper jaws. Combined with their similar gill arches and pharyngeal dentition, this suggests that they may also have similar feeding habits, although the diet of *Hemicaranx* spp. has not been investigated. Could this be a case of morphological convergence associated with trophic ecology as Grubich (2003) has shown for certain durophagic perciforms? If these two genera are indeed sister taxa, then based on their many other character differences and the remarkable external similarity of *Parastromateus* to the Eocene †*Paratrachinotus*, they likely have had a long history of evolutionary separation. These and other characters now must be weighed in light of other aspects of the morphology in an expanded cladistic analysis of the interrelationships of the carangid fishes, including †*Paratrachinotus*.

MATERIAL EXAMINED

The following specimens of *Parastromateus niger* were examined and are indicated as dry skeletons (ds), cleared-and-stained (CS), or alcohol-stored (a) specimens; number of alcohol-preserved specimens radiographed is also provided. Standard lengths (SL) are given if known (those of dry skeletons are approximate): AMNH 98698 (145 mm SL, 1 ds); AMNH 98952 (170 mm SL, 1 ds); AMNH 98953 (170 mm SL, 1 ds); AMNH 98697 (175 mm SL, 1 ds); AMNH 98919 (175 mm SL, 1 ds); AMNH 98951 (175 mm SL, 1 ds); AMNH 98955 (175 mm SL, 1 ds); AMNH 98954 (180 mm SL, 1 ds); AMNH 98957 (180 mm SL, 1 ds); AMNH 98917 (185 mm SL, 1 ds); AMNH 98918 (185 mm SL, 1 ds); AMNH 98949 (185 mm SL, 1 ds); AMNH 214780 (185 mm SL, 1 ds); AMNH 98947 (190 mm SL, 1 ds); AMNH 98948 (190 mm SL, 1 ds); AMNH 98956 (200 mm SL, 1 ds); AMNH 98696 (210 mm SL, 1 ds); AMNH 99021 (255 mm SL, 1 ds); AMNH 99020 (325 mm SL, 1 ds); ANSP 150531 (73.6 mm SL, 1 CS); ANSP 62088 (100–120 mm SL, 3 CS). FMNH 15913 (43–61 mm SL, 4 a, x-ray). MCZ 64462 (132 mm SL, 1 a, x-ray). UF 168246 (102 mm SL, 1 a). USNM 388226 (11 mm SL, 1 CS); USNM

139117 (53 mm SL, 1 a, x-ray); USNM 139119 (56 mm SL, 1 a, x-ray); USNM 316815 (59 mm SL, 1 a, x-ray); USNM 139116 (67 mm SL, 1 a, x-ray); USNM 100297 (82–100 mm SL, 3 a, x-ray); USNM 139118 (118 mm SL, 1 a, x-ray); USNM 307555 (118 mm SL, 1 a, x-ray); USNM 308839 (175 mm SL, 1 a, x-ray); USNM 385517 (205 mm SL, 1 a); USNM 384693 (208 mm SL, 1 a, x-ray).

The following comparative specimens of the Carangoidei were examined. All specimens are cleared and stained.

Coryphaenidae: *Coryphaena hippurus* MCZ 154839 (107 mm SL). Echeneidae: *Echeneis neucratoides* FMNH 117231 (310 mm SL). Nematistiidae: *Nematistius pectoralis* ANSP 148654 (est. 220 mm SL). Rachycentridae: *Rachycentron canadum* MCZ 157656 (157 mm SL). Carangidae: Scomberoidini: *Oligoplites saurus* USNM 383079 (37 mm SL); *Parona signata* ANSP 148655 (184 mm SL); *Scomberoides tala* USNM 36080 (135 mm SL). Trachinotini: *Lichia amia* USNM 383085 (78 mm SL), USNM 383083 (51 mm SL); *Trachinotus carolinus* USNM 383083 (51 mm SL); *Trachinotus ovatus* USNM 319754 (70 mm SL). Naucratini: *Campogramma glaycos* ANSP 135406 (166 mm SL); *Elagatis bipinulata* MCZ 163480 (79 mm SL); *Naucrates ductor* MCZ 164201 (37 mm SL); *Seriola fasciata* MCZ 157674 (109 mm SL); *Seriolina nigrofasciata* ANSP 140622 (est. 132 mm SL). Carangini: *Alectis alexandrinus* USNM 383089 (92 mm SL); *Alepes djedaba* USNM 347148 (110 mm SL); *Atropus atropos* ANSP 144403 (95 mm SL); *Atule mate* USNM 325271 (110 mm SL); *Carangoides plagiotaenia* USNM 362714 (129 mm SL); *Caranx crysos* USNM 158866 (98 mm SL); *Chloroscombrus chrysurus* USNM 383077 (64 mm SL); *Decapterus punctatus* USNM 383086 (108 mm SL); *Gnathanodon speciosus* USNM 383087 (87 mm SL); *Hemicaranx amblyrhynchus* ANSP 139101a (106 mm SL); *Megalaspis cordyla* USNM 347146 (130 mm SL); *Pantolabus radiatus* ANSP 147709 (122 mm SL); *Parastromateus niger* (see above); *Pseudocaranx dentex* USNM 222104 (127 mm SL); *Selar crumenophthalmus* MCZ 149687 (56 mm SL); *Selaroides leptolepis* MCZ 59266 (65 mm SL); *Selene vomer* USNM 383081 (54 mm SL); *Trachurus mediterraneus* USNM 383084 (81 mm SL); *Ulua mentalis* USNM 347149 (100 mm SL); *Uraspis* sp. USNM 362716 (100 mm SL).

ACKNOWLEDGMENTS

LITERATURE CITED

Apsangikar, D. K. 1953. The systematic position of *Stromateus niger*. Journal of the University of Bombay, new series 21B:41–50.

Bannikov, A. F. 1987. The phylogenetic relationships of the carangid fishes of the subfamily Caranginae. Paleontological Journal 1987:44–53.

Bannikov, A. F. 1990. Fossil Carangids and Apolectids of the USSR. Nauka Publishers, Moscow. [in Russian]

Bannikov, A. F., and V. F. Fedotov. 1984. The fossil Apolectidae (Perciformes). Journal of Ichthyology 24:156–158.

de Beaufort, L. F., and W. M. Chapman. 1951. The Fishes of the Indo-Australian Archipelago. IX. Percomorphi (concluded), Blennioidea. E. J. Brill, Leiden.

Bleeker, P. 1864. Sixième notice sur la faune ichthyologique de Siam. Nederlandsch Tijdschrift voor de Dierkunde 2:171–176.

Bloch, M. E. 1795. Naturgeschichte der ausländischen Fische. v. 9:1–192, plates 397–429. J. Morino, Berlin.

Cuvier, G., and A. Valenciennes. 1832. Histoire naturelle des poissons. Tome neuvième. Suite du livre neuvième. Des Scombéroïdes 8:i–xix+5 pp. + 1–509, Pls. 209–245.

Dadzie, S. 2007. Food and feeding habits of the black pomfret, *Parastromateus niger* (Carangidae) in the Kuwaiti waters of the Arabian Gulf. Cybium 31:77–84.

Dadzie, S., F. Abou-Seedo, and E. Al-Qattan. 2000. The food and feeding habits of the silver pomfret, *Pampus argenteus* (Euphrasen), in Kuwait waters. Journal of Applied Ichthyology 16:61–67.

Deng, S., G. Q. Xiong, and H. X. Zhan. 1985. On morphological features of the lateral line canal system of Carangidae, with their applications in taxonomic study. Transactions of the Chinese Ichthyological Society 4:41–60.

Deng, S., and H. Zhan. 1986. Comparative studies of the lateral line canal system of families to be related with the Carangidae, p. 561–569. *In*: Indo-Pacific Fish Biology: Proceedings of the Second International Conference on Indo-Pacific Fishes. T. Uyeno, R. Arai, T. Taniuchi, and K. Matsuura (eds.). Ichthyological Society of Japan, Tokyo.

Dingerkus, G., and L. D. Uhler. 1977. Enzyme clearing of alcian blue stained whole small vertebrates for demonstration of cartilage. Journal of Stain Technology 52:229–232.

Doiuchi, R., T. Sato, and T. Nakabo. 2004. Phylogenetic relationships of the stromateoid fishes (Perciformes). Ichthyological Research 51:202–212.

Eschmeyer, W. N., and R. Fricke (eds.). 2008. Catalog of Fishes. Electronic version (updated 18 Dec. 2008). http://research.calacademy.org/ichthyology/catalog/fishcatsearch.html

Friehofer, W. C. 1963. Patterns of the ramus lateralis accessorius and their systematic significance in fishes. Stanford Ichthyological Bulletin 8:81–189.

Friehofer, W. C. 1978. Cranial nerves of a percoid fish, *Polycentrus schomburgkii* (family Nandidae), a contribution to the morphology and classification of the order Perciformes. Occasional Papers of the California Academy of Sciences 128:1–78.

Fritzsche, R. A., and G. D. Johnson. 1980. Early osteological development of white perch and striped bass with emphasis on identification of their larvae. Transactions of the American Fisheries Society 109:387–406.

Fujita, K. 1990. The Caudal Skeleton of Teleostean Fishes. Tokai University Press, Tokyo.

Greenwood, P. H., D. E. Rosen, S. H. Weitzman, and G. S. Myers. 1966. Phyletic studies of teleostean fishes, with a

provisional classification of living forms. Bulletin of the American Museum of Natural History 131:341–455.

Grubich, J. 2003. Morphological convergence of pharyngeal jaw structure in durophagous perciform fish. Biological Journal of the Linnean Society 80:147–165.

Gushiken, S. 1988. Phylogenetic relationships of the perciform genera of the family Carangidae. Japanese Journal of Ichthyology 34:443–461.

Haedrich, R. L. 1967. The stromateoid fishes: systematics and a classification. Bulletin of the Museum of Comparative Zoology 135:31–139.

Haedrich, R. L. 1971. The pons moultoni, a significant character. Copeia 1971:167–169.

Hilton, E. J., and G. D. Johnson. 2007. When two equals three: developmental osteology of the caudal skeleton in carangid fishes (Perciformes: Carangidae). Evolution and Development 9:178–189.

Hollister, G. 1941. Caudal skeleton of Bermuda shallow water fishes. V. Order Percomorphi: Carangidae. Zoologica 26:31–45.

ICZN (International Commission on Zoological Nomenclature). 1999. International Code of Zoological Nomenclature. Fourth edition. International Trust for Zoological Nomenclature, London.

Johnson, G. D. 1984. Percoidei: development and relationships, p. 464–498. *In*: Ontogeny and Systematics of Fishes. H. G. Moser, W. J. Richards, D. M. Cohen, M. P. Fahay, A. W. Kendall, Jr., and S. L. Richardson (eds.). American Society of Ichthyologists and Herpetologists, Lawrence, Kansas.

Johnson, G. D., and R. A. Fritzsche. 1989. *Graus nigra*, an omnivorous girellid, with a comparative osteology and comments on relationships of the Girellidae (Pisces: Perciformes). Proceedings of the Academy of Natural Sciences of Philadelphia 141:1–27.

Jordan, D. S. 1923. A classification of fishes including families and genera as far as known. Stanford University Publications, University Series, Biological Sciences 3:77–243.

Laroche, W. A., W. F. Smith-Vaniz, and S. L. Richardson. 1984. Carangidae: development, p. 510–522. *In*: Ontogeny and Systematics of Fishes. H. G. Moser, W. J. Richards, D. M. Cohen, M. P. Fahay, A. W. Kendall, Jr., and S. L. Richardson (eds.). American Society of Ichthyologists and Herpetologists, Lawrence, Kansas.

Le Danois, Y. 1963. Remarques ostéo-myologiques sur certains poissons de l'ordre des scombres. Mémoires de l'Institute Français d'Afrique Noire 68:109–152.

McCulloch, A. R. 1929. A check-list of the fishes recorded from Australia. Australian Museum Memoirs 5:145–329.

Monod, T. 1968. Le complex urophore des poissons téléostéens. Mémoires de l'Institut Fondamental d'Afrique Noire 81:1–705.

Nelson, G. J. 1969. Gill arches and the phylogeny of fishes, with notes on the classification of vertebrates. Bulletin of the American Museum of Natural History 141:475–552.

Nelson, J. 2006. Fishes of the World. Fourth edition. Wiley, New York.

Nichols, J. T. 1950. *Hildebrandella*, a new generic name for a carangid fish from the Philippines. Copeia 1950:19–21.

Pati, S. 1980. Food and feeding habits of silver pomfret, *Pampus argenteus* (Euphrasen) from Bay of Bengal with a note on its significance in fishery. Indian Journal of Fisheries 27:244–255.

Pati, S. 1983. Observations on the biology and fishery of black pomfret *Parastromateus niger* (Bloch) from the Bay of Bengal. Acta Ichthyologica et Piscatoria 13:63–73.

Patterson, C., and G. D. Johnson. 1995. The intermuscular bones and ligaments of teleostean fishes. Smithsonian Contributions to Zoology 559:1–85.

Reed, D. L., K. E. Carpenter, and M. J. de Gravelle. 2002. Molecular systematics of the jacks (Perciformes: Carangidae) based on mitochondrial cytochrome *b* sequences using parsimony, likelihood, and Bayesian approaches. Molecular Phylogenetics and Evolution 23:513–524.

Regan, C. T. 1902. A revision of the fishes of the family Stromateidae. Annals and Magazine of Natural History series 7:115–131.

Richardson, J. 1846. Report on the ichthyology of the seas of China and Japan. British Association Advancement of Science, Report of the 15th Meeting [1845]: 187–320.

Smale, M. J., G. Watson, and T. Hecht. 1995. Otolith atlas of southern African marine fishes. Ichthyological monograph of the J.L.B. Smith Institute of Ichthyology, No. 1:1–253 + 149 plates.

Smith, J. L. B. 1965. The Sea Fishes of Southern Africa. Fifth edition. Central News Agency, Ltd., Cape Town.

Smith-Vaniz, W. F. 1984. Carangidae: relationships, p. 522–530. *In*: Ontogeny and Systematics of Fishes. H. G. Moser, W. J. Richards, D. M. Cohen, M. P. Fahay, A. W. Kendall, Jr., and S. L. Richardson (eds.). American Society of Ichthyologists and Herpetologists, Lawrence, Kansas.

Smith-Vaniz, W. F. 1986. Carangidae, p. 638–660. *In*: Smith's Sea Fishes. M. M. Smith and P. C. Heemstra (eds.). Springer, Berlin.

Smith-Vaniz, W. F. 1999. Carangidae, Jacks and scads (also trevallies, queenfishes, runners, amberjacks, pilotfishes, pampanos, etc.), p. 2659–2756. *In*: FAO Species Identification Guide for Fishery Purposes. The Living Marine Resources of the Western Central Pacific. Volume 4. Bony Fishes Part 2 (Mugilidae to Carangidae). K. E. Carpenter and V. H. Niem (eds.). FAO, Rome.

Smith-Vaniz, W. F., and J. C. Staiger. 1973. Comparative revision of *Scomberoides*, *Oligoplites*, *Parona*, and *Hypacanthus* with comments on the phylogenetic position of *Campogramma* (Pisces: Carangidae). Proceedings of the California Academy of Sciences fourth series 39: 185–256.

Springer, V. G., and G. D. Johnson. 2004. Study of the dorsal gill-arch musculature of teleostome fishes, with special reference to the Actinopterygii. Bulletin of the Biological Society of Washington 11:1–260, 205 plates.

Springer, V. G., and W. F. Smith-Vaniz. 2008. Supraneural and pterygiophore insertion patterns in carangid fishes, with description of a new Eocene carangid tribe, †Paratrachinotini, and a survey of anterior anal-fin pterygiophore insertion patterns in Acanthomorpha. Bulletin of the Biological Society of Washington 16:1–73.

Starks, E. C. 1911. The osteology and relationships of the fishes belonging to the family Carangidae. Leland Stanford Jr. University Publications, University Series 5:27–49.

Suda, Y. 1996. Osteology and muscular attachments of the Japanese jack mackerel, *Trachurus japonicus*. Bulletin of Marine Science 58:438–493.

Suzuki, K. 1962. Anatomical and taxonomical studies on the carangid fishes of Japan. Report of Faculty of Fisheries Prefectural Univiversity of Mie 4:43–232.

Witzell, W. N. 1978. *Apolectus niger* (family Apolectidae): synonymy and systematics. Matsya 3 [for 1977]: 72–82.

Yamada, U., and T. Nakabo. 1986. Morphology and ecology of *Parastromateus niger* (Bloch) (family Carangidae) from the East China Sea. UO 36:1–14.